23. Y. Kawano, T. Yoshida, K. Hieda, J. Aoki, H. Miyoshi, Y. Koyanagi, J. Virol. **78**, 11352–11359 (2004)
24. H. Kuwata, Y. Watanabe, H. Miyoshi, M. Yamamoto, T. Kaisho, K. Takeda, S. Akira, Blood **102**, 4123–4129 (2003)
25. H. Ebina, J. Aoki, S. Hatta, T. Yoshida, Y. Koyanagi, Microbes Infect. **6**, 715–724 (2004)
26. U.K. von Schwedler, M. Stuchell, B. Muller, D.M. Ward, H.Y. Chung, E. Morita, H.E. Wang, T. Davis, G.P. He, D.M. Cimbora, A. Scott, H.G. Krausslich, J. Kaplan, S.G. Morham, W.I. Sundquist, Cell **114**, 701–713 (2003)
27. H. Miyoshi, U. Blomer, M. Takahashi, F.H. Gage, I.M. Verma, J. Virol. **72**, 8150–8157 (1998)
28. A. Adachi, H.E. Gendelman, S. Koenig, T. Folks, R. Willey, A. Rabson, M.A. Martin, J. Virol. **59**, 284–291 (1986)
29. Z.L. Xu, H. Mizuguchi, T. Mayumi, T. Hayakawa, Gene **309**, 145–151 (2003)
30. H.R. Jayakar, M.A. Whitt, J. Virol. **76**, 8011–8018 (2002)
31. M.R. Mautino, R.A. Morgan, Aids Patient Care STDS **16**, 11–26 (2002)
32. M. Mukhtar, H. Duke, M. BouHamdan, R.J. Pomerantz, Hum. Gene Ther. **11**, 347–359 (2000)
33. M.R. Mautino, R.A. Morgan, Gene Ther. **9**, 421–431 (2002)
34. A. Banerjea, M.J. Li, G. Bauer, L. Remling, N.S. Lee, J. Rossi, R. Akkina, Mol. Ther. **8**, 62–71 (2003)
35. M.J. Li, G. Bauer, A. Michienzi, J.K. Yee, N.S. Lee, J. Kim, S. Li, D. Castanotto, J. Zaia, J.J. Rossi, Mol. Ther. **8**, 196–206 (2003)
36. H. Nishitsuji, T. Ikeda, H. Miyoshi, T. Ohashi, M. Kannagi, T. Masuda, Microbes Infect. **6**, 76–85 (2004)
37. R. Zufferey, J.E. Donello, D. Trono, T.J. Hope, J. Virol. **73**, 2886–2892 (1999)
38. E. Vigna, S. Cavalieri, L. Ailles, M. Geuna, R. Loew, H. Bujard, L. Naldini, Mol. Ther. **5**, 252–261 (2002)
39. R. Vogel, L. Amar, A.D. Thi, P. Saillour, J. Mallet, Hum. Gene Ther. **15**, 157–165 (2004)

Microbiology and Immunology

Microbiol Immunol 2009; **53**: 629–635
doi:10.1111/j.1348-0421.2009.00167.x

ORIGINAL ARTICLE

N-linked glycan-dependent interaction of CD63 with CXCR4 at the Golgi apparatus induces downregulation of CXCR4

Takeshi Yoshida, Hirotaka Ebina and Yoshio Koyanagi

Laboratory of Viral Pathogenesis, Institute for Virus Research, Kyoto University, Sakyo-ku, Kyoto, 606-8507, Japan

ABSTRACT

Efficient downregulation of CXCR4 cell surface expression by introduction of the CD63 gene has previously been reported by us. In the present study, it was found that CD63 and its mutant efficiently interact with CXCR4 in live cells and that CD63-induced downregulation and interaction are significantly abrogated by the *N*-linked glycosylation inhibitor, TM. Furthermore, the downregulation and interaction were clearly attenuated by alternation of all three *N*-linked glycosylation sites in CD63. Either CD63 or CD63ΔN formed a complex with CXCR4 at the Golgi apparatus and the late endosomes, while CD63 GD mutants lost the ability to form a complex with CXCR4 exclusively at the Golgi apparatus. These findings suggest that CD63 interacts with CXCR4 through the *N*-linked glycans-portion of the CD63 protein and that the complex induces direction of CXCR4 trafficking to the endosomes/lysosomes, rather than to the plasma membrane. At the Golgi apparatus, there may be lysosome protein (CD63)-associated machinery that influences trafficking of other membrane proteins.

Key words CXCR4, membrane trafficking, *N*-linked glycosylation, tetraspanin.

At the Golgi apparatus, the cellular sorting machineries govern directing of secretory proteins to either the plasma membrane or to the endosomal system (1). The secretory pathway links organelles together to provide a framework by which proteins undergo a series of posttranslational modifications including folding and glycosylation. *N*-linked glycosylation of proteins is known to be related to chaperone-mediated folding of the polypeptide, thus contributing to quality control in the ER (2). However, it remains unknown whether *N*-linked glycans take part in physiological events within other intracellular compartments.

We previously found that tetraspanin CD63 has an opposing effect on the expression of the chemokine receptor CXCR4(3). CD63ΔN induces severe downregulation of CXCR4 surface expression, and this effect appears to be caused by selective direction of CXCR4 from the Golgi apparatus to the endosomes/lysosomes, rather than to the plasma membrane (3). This suggests that CD63ΔN, probably CD63 itself, might have a role in the control of CXCR4 trafficking to different final destinations.

We show herein that the *N*-linked glycans-portion of CD63 functions as a determinant of alteration of CXCR4 trafficking.

MATERIALS AND METHODS

Expression plasmids

pCXCR4-mKGC (4), phmKGN-MC, (Medical & Biological Laboratories, Nagoya, Japan), pcDNA3.1 and pCMV-SPORT6 (Invitrogen, Carlsbad, CA, USA) were used.

Correspondence
Yoshio Koyanagi, Laboratory of Viral Pathogenesis, Institute for Virus Research, Kyoto University, 53 Shogoin-kawara-cho, Sakyo-ku, Kyoto, 606-8507, Japan.
Tel: 81 75 751 4811; fax: 81 75 751 4812; email: ykoyanag@virus.kyoto-u.ac.jp

Received 21 April 2009; revised 7 July 2009; accepted 20 July 2009.

List of Abbreviations: BiFC, bimolecular fluorescence complementation; CD63ΔN, an N-terminal deletion mutant of CD63; CD63FL, CD63 full length; ceramide, NBD C_5-ceramide; DIC, differential interference contrast; ER, endoplasmic reticulum; FL, full length; GD, *N*-linked glycans-deficient form; GI, glycans-intact form; KG, Kusabira green; KGC-CXCR4, C-terminal KG peptide-tagged CXCR4; KGN-CD63ΔN, N-terminal KG peptide-tagged CD63ΔN; MFI, mean fluorescence intensity; TGN, trans-Golgi network; TM, tunicamycin.

Plasmid DNA expressing GD mutants substituted from Asn to Glu at three *N*-linked glycosylation sites (amino acid position at 130, 150 and 172) of CD63ΔN and CD63FL were generated by overlap extension PCR. An orf fragment of *CD63FL, CD63ΔN* or these GD mutants was inserted into pCMV-SPORT6, downstream sites of N-terminal KGN peptide-tag in phmKGN-MC or FLAG-tag in p3XFLAG-CMV-10 (Sigma, St Louis, MO, USA). An HA-tag was inserted into an upstream site of the CD63 orf fragment in pCMV-SPORT6 by PCR. pCXCR4 is made from SRαLEGFP (5) by replacement of *EGFP* with *CXCR4*. The nucleotide sequences of all plasmids were confirmed using ABI 3100 auto-sequencer.

Cell culture and transfection

293T, MAGIC-5 and MT-4 cells were used as previously described (3). A transIT LT-1 transfection reagent (Mirus Bio, Madison, WI, USA) and the calcium phosphate method were used for DNA transfection into MAGIC-5 and 293T cells, respectively. To measure the extent of suppression of CXCR4 surface expression, 293T cells were co-transfected with either 0.5 μg of GI or 1.5 μg of GD of CD63ΔN plasmid DNA, or either 0.05 μg of GI or 0.15 μg of GD of CD63FL plasmid DNA together with 2 μg of pCXCR4.

Lentiviral vector transduction and HIV-1 infection

A bicistronic $H2K^k$-expressing lentiviral vector and HIV-1 envelope-pseudotyped luciferase-expressing $HIV\text{-}1_{NL-4}$ (NL-luc) were prepared and used as described previously (3,6,7).

Flow cytometry

Staining of CXCR4 was performed as previously described (3). For BiFC assay (8), cells were transfected with 0.5 μg of KGN-tagged GI or 1.5 μg of GD of either CD63FL or CD63ΔN plasmid DNA together with 0.5 μg of pCXCR4-mKGC. Culture media was replaced by media with or without 0.5 μM of TM (Sigma-Aldrich, St. Louis, MO, USA) 12 hr post transfection.

Immunoblotting

CXCR4 and β-actin were detected as previously described (3). Anti-CD63 mAb (Santa Cruz Biotechnology) and anti-KGN mAb (Medical and Biological Laboratories) were also used.

Microscopic analyses

FLAG- and HA-protein, p230, and LAMP-1 were detected as previously described (3). Anti-HA mAb (3F10, Roche, Indianapolis, IN, USA) was used. For live cell imaging, transfected cells were stained with ceramide, Hoechst33342 (Molecular Probes, Eugene, OR, USA) or LysoTracker Blue DND-22 (Molecular Probes). Cells were analyzed using a DMIRE2-TCS SP2 AOBS confocal microscope system (Leica, Heidelberg, Germany) and images were processed using Photoshop CS2 (Adobe).

Statistical analysis

The Mann–Whitney's *U* test and Student's *t*-test were used to determine statistical significance.

RESULTS

Requirement of N-linked glycans of CD63 for downregulation of CXCR4

We initially confirmed clear downregulation of CXCR4 surface expression in CD63ΔN- or CD63FL-transduced MT-4 cells compared to that in empty vector-transduced cells (Fig. 1a, columns of 1 in top) as described previously (3). Next, we examined the effect of an *N*-linked glycosylation inhibitor, TM, on surface expression of CXCR4. Following 12 hr TM treatment, CXCR4 surface expression increased in CD63ΔN- or CD63FL-transduced cells but not in empty vector-transduced cells (Fig. 1a, top columns). Glycosylation of endogenous CD63, ectopically expressed CD63ΔN and CD63FL in the cells were clearly inhibited by TM treatment (Fig. 1a, upper panels). On the other hand, we found similar CXCR4 bands irrespective of TM treatment (Fig. 1a, middle panels). Because the kinetics of newly synthesized CD63 is faster than that of CXCR4 (9,10), following TM treatment glycosylated CD63 seemed to disappear more quickly than glycosylated CXCR4. In addition, we also observed more significant abrogation of CXCR4 downregulation following TM treatment in CD63ΔN-transduced MAGIC-5 cells (Fig. 1b). Since the surface expression of CXCR4 GD mutants is, however, known to be comparable to that of the wild type (11), it is possible that *N*-linked glycosylation in ectopically expressed CD63ΔN and CD63FL is indispensable for CXCR4 downregulation.

To assess this possibility, we generated plasmid DNA expressing GD mutants of CD63ΔN and CD63FL whose three potential *N*-liked glycosylation Asn sites (amino acid position at 130, 150 and 172) were respectively or together substituted with Gln. Western blotting of cells transfected with these GD mutant DNA showed smaller bands compared to those with GI DNA, indicating that all three sites are glycosylated (data not shown). When cells were co-transfected with pCXCR4 and the individual plasmid DNA of these GD mutants, we observed clearly less

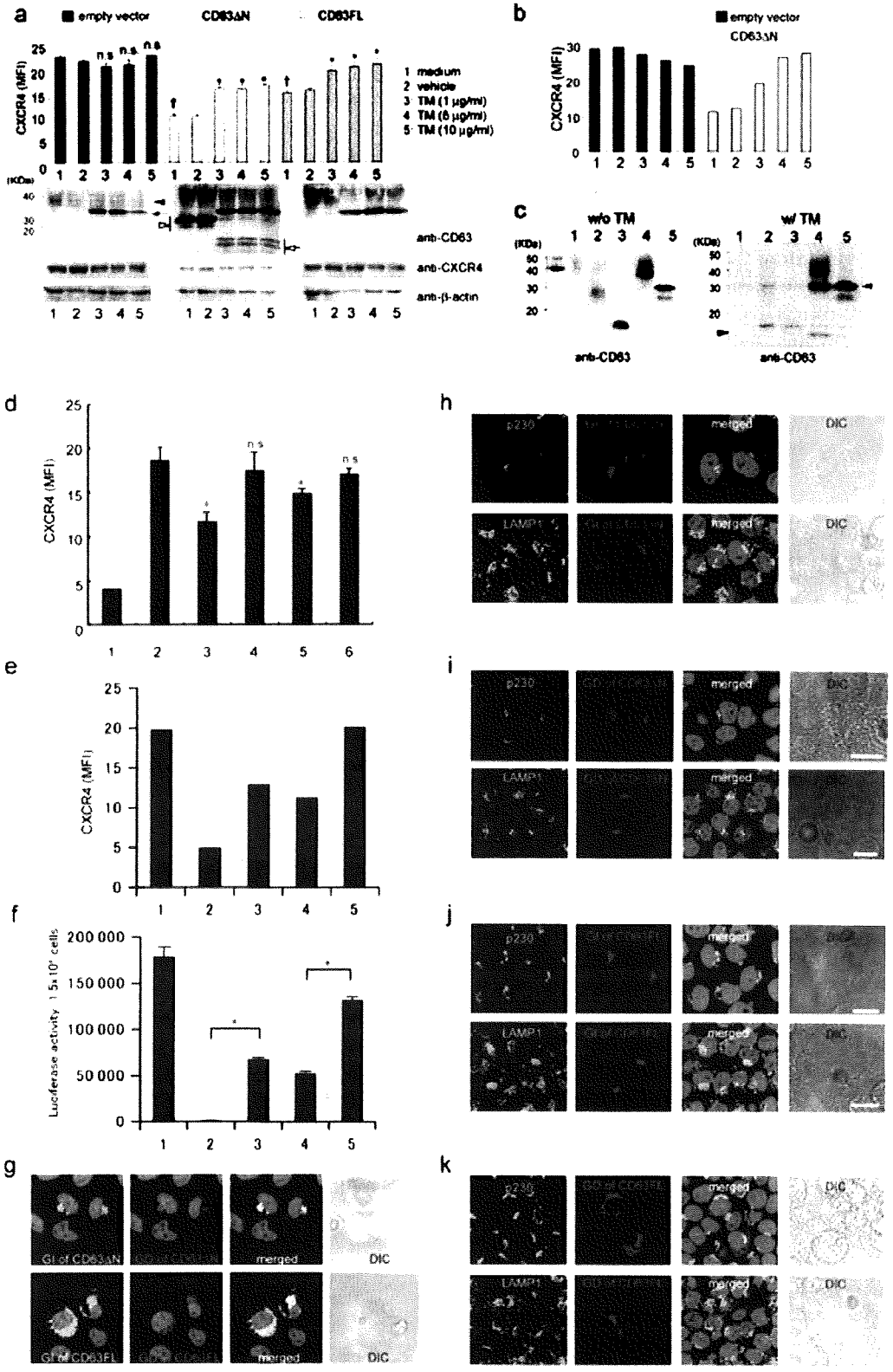

Fig. 1. The importance of the *N*-linked glycans of CD63 for downregulation of CXCR4. (a) Flow cytometric analysis of CXCR4 (MFI in top columns) and Western blotting (lower three panels). Lentiviral vector-transduced MT-4 cells were treated with TM as indicated. Data are represented as mean ±SED, $n = 3$. (Black arrow head) glycosylated CD63FL; (black arrow) unglycosylated CD63FL; (white arrow head) glycosylated CD63ΔN;

downregulation of CXCR4 only in the GD mutants that were substituted at all three *N*-liked glycosylation sites of CD63ΔN and CD63FL though the extent of mutant expression was slightly less as shown by Western blotting (data not shown). To normalize the expression, we transfected cells with more plasmid DNA of GD than that of GI. When the ratio of the DNA of GD to GI was 3 to 1 for CD63FL and CD63ΔN, we obtained an equivalent level of protein expression (Fig. 1c, lanes 2 vs. 3 and 4 vs. 5). Under this condition, we found efficient capability in downregulation for transiently expressed CXCR4 in plasmid DNA expressing GI of CD63ΔN or CD63FL (Fig. 1d, columns 3 and 5), but not in plasmid DNA expressing GD of CD63ΔN or CD63FL (Fig. 1d, columns 4 and 6). The downregulation ability of CD63 GD-expressing lentiviral vectors for endogenous CXCR4 was also clearly attenuated compared to that of CD63 GI-expressing lentiviral vectors (Fig. 1e, lane 2 vs. 3 and 4 vs. 5) under its equivalent transduction efficiency of the lentiviral vectors as shown by staining with anti-$H2K^K$ antibody (data not shown). However, the extent of CXCR4 surface expression on CD63ΔN GD-transduced MT-4 cells was still less than that on empty vector-transduced MT-4 cells.

Correlating to the CXCR4 surface expression on these transduced cells, the HIV-1 susceptibility of GD-transduced MT-4 cells, (examined by CXCR4-using HIV-1 envelope-pseudotyped NL-luc), was clearly greater than that of GI-transduced MT-4 cells (Fig. 1f). On the other hand, distribution of GD mutants in cells was almost identical to that of GI proteins, as shown by dual staining of GI and GD in cells co-transfected with plasmid DNA expressing GD and GI of CD63ΔN and CD63FL (Fig. 1g). In addition, experiments involving staining of GI or GD of CD63ΔN and CD63FL together with antibody against p230 (the TGN marker) or LAMP-1 (the late endosome marker) confirmed that intracellular localization of the GD mutants was unchanged (Fig. 1h–k). Collectively, these data indicate that the *N*-linked glycans-portion of CD63ΔN and CD63FL, not its distribution, may be required for limiting CXCR4 surface expression.

N-linked glycans-dependent interaction of CD63 with CXCR4

We previously detected interaction of CD63ΔN or CD63FL with CXCR4 by immunoprecipitation-Western blotting (3). To confirm the interactions in live cells, we next used a BiFC assay to enable us to visualize the intracellular distribution of specific interactive complexes (8). MAGIC-5 cells were co-transfected with plasmid DNA expressing KGC-CXCR4 and either KGN-CD63ΔN or KGN-CD63FL. We detected CXCR4-CD63ΔN complexes exclusively in the perinuclear regions (Fig. 2a, upper panel), and they appeared to be predominantly distributed at the ceramide$^+$ region (the Golgi apparatus) and LysoTracker$^+$ region (the late endosomes/lysosomes) (Fig. 2a), suggesting that CD63ΔN interacts with CXCR4 mainly at the Golgi apparatus and the late endosomes/lysosomes. In contrast, CXCR4-CD63FL complexes were detected at the plasma membrane as well as in the perinuclear regions (Fig. 2b, upper panel). The perinuclear CXCR4-CD63FL complexes were positively stained with ceramide and Lyso Tracker (Fig. 2b). Thus, the CXCR4-CD63ΔN complex seems to lose the ability to be trafficked to the plasma membrane. When cells were co-transfected with plasmid DNA expressing KGC-CXCR4 and GD of KGN-CD63ΔN, we found significant decrease in signal, which was very

Fig. 1. (white arrow) unglycosylated CD63ΔN; (n.s.) $P > 0.01$ compared to same cells treated with vehicle; (*) $P < 0.01$ compared to same cells treated with vehicle; (†) $P < 0.01$ compared to untreated empty vector-transduced cells. (**b**) Flow cytometric analysis of CXCR4. Lentiviral vector-transduced MAGIC-5 cells were treated as indicated in (a). (**c**) Western blotting of GI and GD of CD63ΔN or CD63FL. 293T cells were transfected with empty vector (lane 1), plasmid DNA expressing GI of CD63ΔN (lane 2), GD of CD63ΔN (lane 3), GI of CD63FL (lane 4), GD of CD63FL (lane 5) and probed with the indicated mAb. (Black arrow head) unglycosylated form of CD63ΔN; (white arrow head) unglycosylated form of CD63FL. (**d**) Flow cytometric analysis of exogenous CXCR4. 293T cells were co-transfected without pCXCR4 and empty vector (column 1), with pCXCR4 and empty vector (column 2), plasmid DNA expressing GI of CD63ΔN (column 3), GD of CD63ΔN (column 4), GI of CD63FL (column 5), GD of CD63FL (column 6) and analyzed 24 hr post transfection. Data are represented as mean ±SED, $n = 6$. (n.s.), $P > 0.01$ as compared to column 2; (*), $P < 0.01$ as compared to column 2. (**e**) Flow cytometric analysis of endogenous CXCR4. (**f**) HIV-1 susceptibility. MT-4 cells were transduced by lentiviral vector of empty vector (column 1), GI of CD63ΔN (column 2), GD of CD63ΔN (column 3), GI of CD63FL (column 4), GD of CD63FL (column 5). (**e, f**) CXCR4 surface expression on these cells and HIV-1 susceptibility was analyzed as described before (3,7). $n = 3$. (*) $P < 0.01$ as compared to column 2 or 4. (**g–k**) Confocal microscopic analysis of GI and GD of CD63ΔN or CD63FL. (**g**) MAGIC-5 cells were co-transfected with either GI of FLAG-CD63ΔN and GD of HA-CD63ΔN plasmid DNA (upper panels) or GI of FLAG-CD63FL and GD of HA-CD63FL plasmid DNA (lower panels) and co-stained with anti-HA and anti-FLAG mAbs. (Red) FLAG-protein; (green) HA-protein; (blue) nuclei. DIC images are also shown. Scale bar, 10 μm. Cells were transfected (**h**) with GI of FLAG-CD63ΔN, (**i**) with GD of FLAG-CD63ΔN, (**j**) with GI of FLAG-CD63FL, or (**k**) with GD of FLAG-CD63FL. These cells were co-stained with antibodies against FLAG (red) and p230 or LAMP-1. (**h-k**). Scale bars, 20 μm.

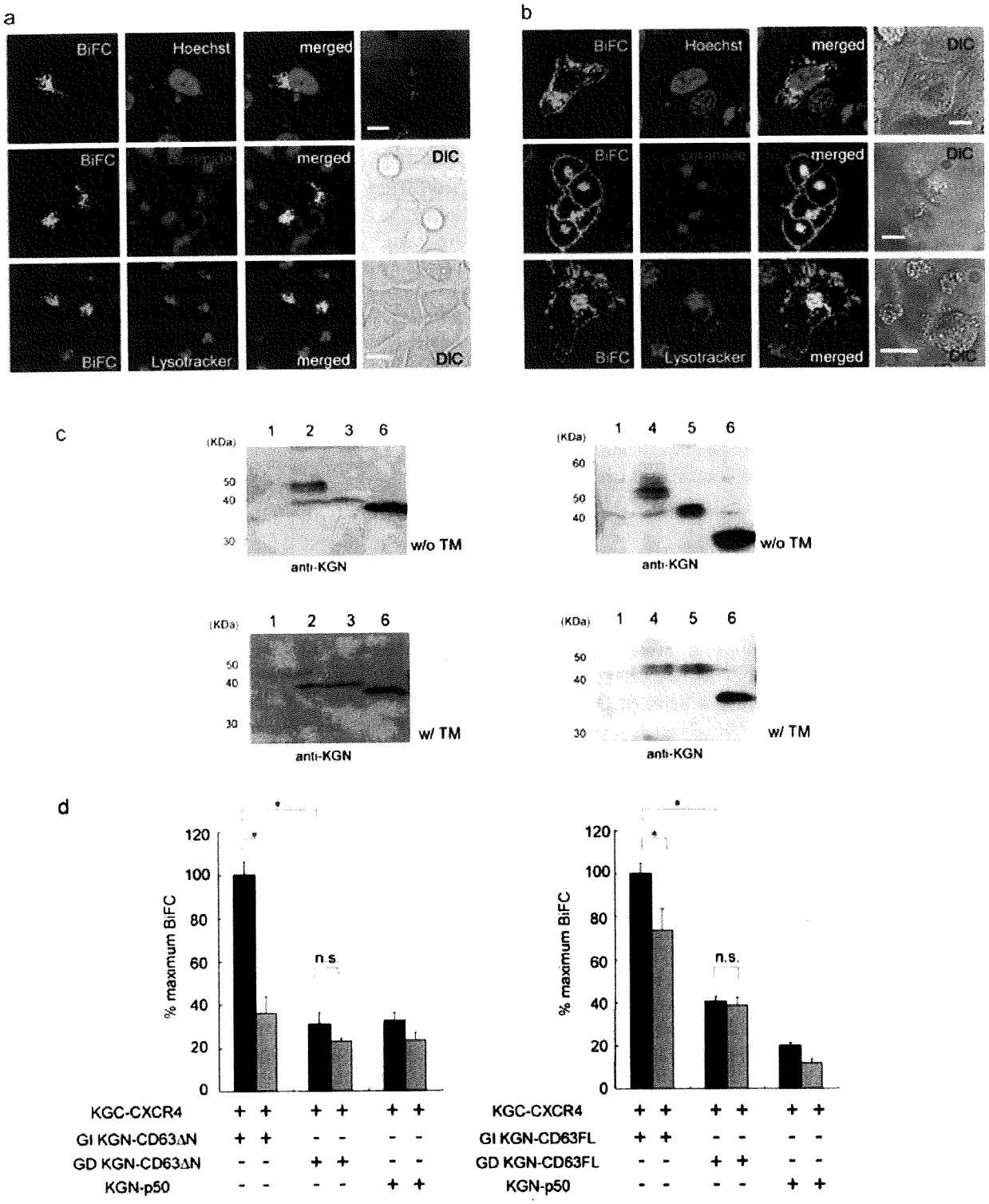

Fig. 2. *N*-linked glycans-dependent interaction of CD63 with CXCR4. (**a**,**b**) BiFC analysis of interaction of CXCR4 with (a) CD63ΔN or (b) CD63FL as shown by confocal microscopy. Scale bars, 10 μm. DIC images are also shown. (**c**) Western blotting of GI and GD of KGN-CD63ΔN or KGN-CD63FL. 293T cells were transfected with pcDNA3.1 (lane 1), plasmid DNA expressing GI of KGN-CD63ΔN (lane 2), GD of KGN-CD63ΔN (lane 3), GI of KGN-CD63FL (lane 4), GD of KGN-CD63FL (lane 5), KGN-p50 (lane 6) and probed with the indicated mAb. (**d**) BiFC analysis of CXCR4 and CD63ΔN or CD63FL measured by flow cytometry. 293T cells were co-transfected with plasmid DNA expressing KGC-CXCR4 and KGN-tagged protein as indicated and cultured in the absence (filled columns) or presence (grey columns) of TM. Y axis

weak and predominantly located at the Lyso Tracker$^+$ region and not the ceramide$^+$ region (data not shown). A similar decrease in signal at the ceramide$^+$ region was also found in the case of the CXCR4-GD of CD63FL complex (data not shown).

To quantify the extent of the interaction, we measured the correlative increase in intensity of the fluorescence signal detected in transfected 293T cells by flow cytometry as increase in plasmid DNA expressing KGN-tagged p50 (an NF-κB subunit) and KGC-tagged p65 (a known interaction protein of p50) but not other unrelated molecules (data not shown), indicating that the intensity of the signal using a single pair of expression plasmids reflects the extent of molecular interaction. Comparison of the BiFC signal of CXCR4-CD63FL (GI and GD) with CXCR4-CD63ΔN (GI and GD) was not evaluated due to the difference in strength of the fluorophore constituent. CXCR4-CD63FL (GI and GD) interaction leads to a more stable fluorophore which emits a stronger signal than the one obtained from the CXCR4-CD63ΔN (GI and GD) interaction, making direct comparisons between associations of CD63FL and CD63ΔN inequitable. Therefore, differences between GI and GD of CXCR4-CD63FL only, or with CXCR4-CD63ΔN only, were assessed.

Under normalized conditions on the expression of GI and GD of KGN- CD63ΔN or KGN-CD63FL (Fig. 2c), we found significant fluorescence between CXCR4 and GI of either CD63ΔN or CD63FL (Fig. 2d), whereas less of a fluorescence signal between CXCR4 and GD of either CD63ΔN or CD63FL was observed (Fig. 2d). We also found significant attenuation in the interaction of CXCR4 with GI of either CD63ΔN or CD63FL by TM treatment, but no change in the signal in interactions between CXCR4 with GD of either CD63ΔN or CD63FL, respectively (Fig. 2d, grey columns), indicating that the *N*-linked glycans-portion of CD63ΔN and CD63FL participates in its efficient interaction with CXCR4. Interestingly, although TM treatment of GI of CD63FL and CD63ΔN attenuated the BiFC signal, interaction with CXCR4 was still observed (Fig. 2d). Moderate interaction was also observed in GD mutants regardless of TM treatment. Taken together, these results indicate that even with abrogation of glycosylation, weak interaction between CXCR4 and CD63FL or CD63ΔN may still occur, however not enough to downregulate the receptor.

DISCUSSION

In the present study, we show that the *N*-linked glycans of CD63 protein mediate its interaction with CXCR4 and that this complex formation can convert the destination of CXCR4 to the late endosomes/lysosomes.

To understand the characteristics of the *N*-linked glycans of CD63, we carried out a series of experiments using both CD63FL and CD63ΔN because CD63FL is a native form of the protein and the effect of CD63ΔN on CXCR4 surface expression is more significant than that of CD63FL ((3) and Fig. 1a). First, we showed that the *N*-linked glycans-portion of CD63FL and CD63ΔN is required to induce efficient downregulation of CXCR4 surface expression (Fig. 1d and e) and to interact with CXCR4 (Fig. 2d). It is well known that glycosylation of membrane protein is a crucial step for its correct folding. However, we clearly detected significant expression of GD of CD63ΔN and CD63FL (Fig. 1c, i, and k). Interestingly, other tetraspanins such as CD9 and CD81, which have no potential glycosylation site, had little suppressive activity for CXCR4 surface expression (3), suggesting that *N*-linked glycans-dependent tetraspanin binding to CXCR4 has a role in regulation of CXCR4 trafficking.

CD63 is well known as a marker of the late endosome/lysosome. Furthermore, we showed that CD63ΔN or CD63FL, including GD mutants, localizes in the TGN (Fig. 1h–k). Correspondingly, CD63 has recently been reported to also localize in the TGN and post-TGN-derived vacuoles (12). Another group has also shown that, in contrast to other secretory proteins, there is a distinct processing period for CD63 maturation in the Golgi apparatus (13). Because we detected significant localization of CD63-CXCR4 complexes at the Golgi apparatus (Fig. 2b), it is possible that Golgi-localized CD63 may have an undiscovered role, such as organizing the destination of other proteins.

We originally found CD63ΔN-CXCR4 or CD63FL-CXCR4 complexes by biochemical methods (3) and confirmed their presence in live cells using the BiFC technique (Fig. 2a and b). According to results of transient co-transfection experiments using the same amount of plasmid DNA, the level of CXCR4-CD63ΔN BiFC signal seemed to be weaker than that of CXCR4-CD63FL. Due to differences in the orientation of the BiFC fragments, compared to CD63FL and CXCR4, the MFI produced by

Fig. 2. indicates % of maximum BiFC, which is defined by dividing the MFI values of BiFC interactions by the maximum obtainable MFI from the interaction between CXCR4 and GI of CD63ΔN (left panel) or CD63FL (right panel) in the absence of TM. Data are represented as mean ±SED, $n = 4$. (n.s.), $P > 0.01$; (*), $P < 0.01$.

the interaction of CD63ΔN with CXCR4 may not be able to reach the same maximum intensity. Perhaps the interaction between CD63FL and CXCR4 allows for a more stable fluorophore constitution, whereas the interaction between CD63ΔN and CXCR4 doesn't as a result of different binding affinities or conformational changes of the FL versus the deletion mutant interaction with CXCR4. Therefore, we plotted the two interaction pairs separately and showed that, when compared to the GI CD63 variants not treated with TM, interaction with CXCR4 was significantly reduced when GD CD63 variants were transfected instead of GI CD63FL or CD63ΔN (Fig. 2d).

Detection of the CD63FL-CXCR4 complex at the plasma membrane (Fig. 2b) suggests the possibility that CXCR4 is transported together with CD63 protein. Trafficking efficiency of the CD63FL-CXCR4 complex to the plasma membrane seems to be more significant than that of the CD63ΔN-CXCR4 one. This preferential trafficking of CD63FL may explain the weaker activity of CD63FL for CXCR4 downregulation.

ACKNOWLEDGMENTS

We thank the many colleagues who have contributed ideas and help to this project, in particular Dr. Jun Komano, Mr. Peter Gee for discussion and Ms. Misawa for assistance. This work was supported by grants from the Ministry of Health, Labor, and Welfare and the Ministry of Education, Culture, Sports, Science and Technology of JAPAN. T. Y. is a research fellow of the Japan Society for the Promotion of Science.

REFERENCES

1. van Vliet C., Thomas E.C., Merino-Trigo A., Teasdale R.D., Gleeson P.A. (2003) Intracellular sorting and transport of proteins. *Prog Biophys Mol Biol* **83:** 1–45.
2. Zhao Y.Y., Takahashi M., Gu J.G., Miyoshi E., Matsumoto A., Kitazume S., Taniguchi N. (2008) Functional roles of N-glycans in cell signaling and cell adhesion in cancer. *Cancer Sci* **99:** 1304–10.
3. Yoshida T., Kawano Y., Sato K., Ando Y., Aoki J., Miura Y, Komano J., Tanaka Y., Koyanagi Y. (2008) A CD63 mutant inhibits T-cell tropic human immunodeficiency virus type 1 entry by disrupting CXCR4 trafficking to the plasma membrane. *Traffic* **9:** 540–58.
4. Hamatake M., Aoki T., Futahashi Y., Urano E., Yamamoto N., Komano J. (2009) Ligand-independent higher-order multimerization of CXCR4, a G-protein-coupled chemokine receptor involved in targeted metastasis. *Cancer Sci* **100:** 95–102.
5. An D.S., Koyanagi Y., Zhao J.Q., Akkina R., Bristol G., Yamamoto N., Zack J.A., Chen I.S.Y. (1997) High-efficiency transduction of human lymphoid progenitor cells and expression in differentiated T cells. *J Virol* **71:** 1397–404.
6. Kawano Y., Yoshida T., Hieda K., Aoki J., Miyoshi H., Koyanagi Y. (2004) A lentiviral cDNA library employing lambda recombination used to clone an inhibitor of human immunodeficiency virus type 1-induced cell death. *J Virol* **78:** 11352–59.
7. Sato K., Aoki J., Misawa N., Daikoku E., Sano K., Tanaka Y., Koyanagi Y. (2008) Modulation of human immunodeficiency virus type 1 infectivity through incorporation of tetraspanin proteins. *J Virol* **82:** 1021–33.
8. Ghosh I., Hamilton D., Regan L. (2000) Antiparallel leucine zipper-directed protein reassembly: Application to the green fluorescent protein. *J Am Chem Soc* **122:** 5658–9.
9. Rous B.A., Reaves B., Ihrke G., Briggs J.A., Gray S.R., Stephens D.J., Banting G., Luzio J.P. (2002) Role of adaptor complex AP-3 in targeting wild-type and mutated CD63 to lysosomes. *Mol Biol Cell* **13:** 1071–82.
10. Marchese A., Benovic J.L. (2001) Agonist-promoted ubiquitination of the G protein-coupled receptor CXCR4 mediates lysosomal sorting. *J Biol Chem* **276:** 45509–12.
11. Huskens D., Princen K., Schreiber M., Schols D. (2007) The role of N-glycosylation sites on the CXCR4 receptor for CXCL-12 binding and signaling and X4 HIV-1 viral infectivity. *Virology* **36:** 280–7.
12. Mori Y., Koike M., Moriishi E., Kawabata A., Tang H., Oyaizu H., Uchiyama Y., Yamanishi K. (2008) Human herpesvirus-6 induces MVB formation, and virus egress occurs by an exosomal release pathway. *Traffic* **9:** 1728–42.
13. Ageberg M., Lindmark A. (2003) Characterisation of the biosynthesis and processing of the neutrophil granule membrane protein CD63 in myeloid cells. *Clin Lab Haematol* **25:** 297–306.

T Cell–Mediated Control of Epstein-Barr Virus Infection in Humanized Mice

Misako Yajima,[1] Ken-Ichi Imadome,[1] Atsuko Nakagawa,[2] Satoru Watanabe,[3] Kazuo Terashima,[4] Hiroyuki Nakamura,[1] Mamoru Ito,[6] Norio Shimizu,[3] Naoki Yamamoto,[5] and Shigeyoshi Fujiwara[1]

[1]Department of Infectious Diseases, National Research Institute for Child Health and Development, and [2]Pathology Laboratory, Department of Clinical Laboratory Medicine, National Center for Child Health and Development, Setagaya-ku, [3]Department of Virology, Division of Medical Science, Medical Research Institute, and [4]Department of Pathology, Faculty of Medicine, Tokyo Medical and Dental University, Bunkyo-ku, and [5]AIDS Research Center, National Institute of Infectious Diseases, Shinjuku-ku, Tokyo, and [6]Central Institute for Experimental Animals, Kawasaki, Kanagawa, Japan

Humanized NOD/Shi-*scid*/interleukin-2Rγ^{null} (NOG) mice with full T cell development had significantly longer life span after Epstein-Barr virus (EBV) infection, compared with those with minimal T cell development. Removing CD3$^+$ or CD8$^+$ T cells from EBV-infected humanized mice by administration of anti-CD3 or anti-CD8 antibodies reduced their life span. CD8$^+$ T cells obtained from EBV-infected mice suppressed the outgrowth of autologous B cells isolated from uninfected mice and inoculated with EBV in vitro. These results indicate that humanized NOG mice are capable of T cell–mediated control of EBV infection and imply their usefulness as a tool to evaluate immunotherapeutic and prophylactic strategies for EBV infection.

Epstein-Barr virus (EBV) is a ubiquitous B-lymphotropic herpesvirus, and >90% of the adult population in the world is latently infected with the virus [1]. Although EBV is an important etiological factor in various malignancies, including endemic Burkitt lymphoma, Hodgkin lymphoma, and nasopharyngeal carcinoma, most EBV infection is asymptomatic and persists for life without any signs or symptoms. EBV has a unique ability to transform human B lymphocytes in vitro and to establish immortalized lymphoblastoid cell lines [2]. EBV-transformed lymphoblastoid cell lines express 9 viral proteins, most of which serve as efficient targets of EBV-specific T cell responses [2]. In immunologically competent hosts, therefore, EBV-transformed cells are readily removed by EBV-specific cytotoxic T lymphocytes [3], and EBV persistence is restricted to memory B cells, in which the expression of all viral proteins is shut down [4]. In immunocompromised hosts, however, EBV-infected B lymphoblasts can proliferate to cause lymphoproliferative disorder [1]. Thus, EBV persistence in human hosts is based on a fine balance between the host immunosurveillance, especially the function of EBV-specific cytotoxic T lymphocytes, and the replicative potential of EBV and the growth potential of EBV-infected cells.

Recently, we developed a new humanized mouse model of EBV infection, based on the NOD/Shi-*scid*/interleukin-2Rγ^{null} (NOG) mouse strain [5], that can reproduce key aspects of human EBV infection, such as lymphoproliferative disorder, asymptomatic persistent infection, and humoral and T cell–mediated immune responses [6]. In this model, inoculation with high-dose EBV (~1×10^3 50% transformation dose [TD_{50}]) resulted in the development of lymphoproliferative disorder, whereas inoculation with low-dose virus ($\leq 1 \times 10^1$ TD_{50}) tended to cause apparently asymptomatic persistent infection. Enzyme-linked immunospot assay and flow cytometry identified CD8$^+$ T cells that recognize autologous EBV-transformed lymphoblastoid cells and produce IFN-γ in a human major histocompatibility complex class I–restricted manner [6]. Although immune responses to EBV have been demonstrated in this NOG mouse model and other types of humanized mice [7, 8], whether these immune responses work functionally to control EBV infection has not been clarified. To address this issue, we examined whether T cells in humanized NOG mice have any influence on the survival of EBV-infected mice. We also tested whether CD8$^+$ T cells isolated from EBV-infected NOG mice have a capacity to suppress EBV-induced lymphocyte transformation.

Methods. NOG mice were obtained from the Central Institute for Experimental Animals, and cord blood samples were supplied by the Tokyo Cord Blood Bank after obtaining informed consent. Reconstitution of human immune system components was performed as described elsewhere [6, 9, 10]. In brief, CD34$^+$ human hematopoietic stem cells (HSCs) were isolated from cord blood with use of the MACS Direct CD34 Progenitor Cell Isolation Kit (Miltenyi Biotec), and 1×10^4–

Received 14 May 2009; accepted 19 June 2009; electronically published 15 October 2009.
Potential conflicts of interest: none reported.
Financial support: Ministry of Health, Labour and Welfare of Japan (H19-AIDS-003 and H21-AIDS-008) and a grant for the Research on Publicly Essential Drugs and Medical Devices from The Japan Health Sciences Foundation.
Reprints or correspondence: Dr. Shigeyoshi Fujiwara, Dept. of Infectious Diseases, National Research Institute for Child Health and Development, 2-10-1 Okura, Setagaya-ku, Tokyo 157-8535, Japan (shige@nch.go.jp).
The Journal of Infectious Diseases 2009;200:1611–15

0022-1899/2009/20010-0018$15.00
DOI: 10.1086/644644

1.2×10^5 cells/mouse of HSCs were transplanted in 6–10-week-old female NOG mice via the tail vein. The development of human blood cells in the peripheral blood was monitored by staining with monoclonal antibodies specific to human CD45RA, CD45RO, CD19, CD3, CD4, and CD8. NOG mice in which the human hematoimmune system was reconstituted are referred to here as humanized NOG mice. The term "lot" signifies a group of humanized mice derived from a single cord blood donor. Protocols of experiments with NOG mice were approved by the Institutional Animal Care and Use Committee of the National Institute of Infectious Diseases. The use of human materials in this research was approved by the In-

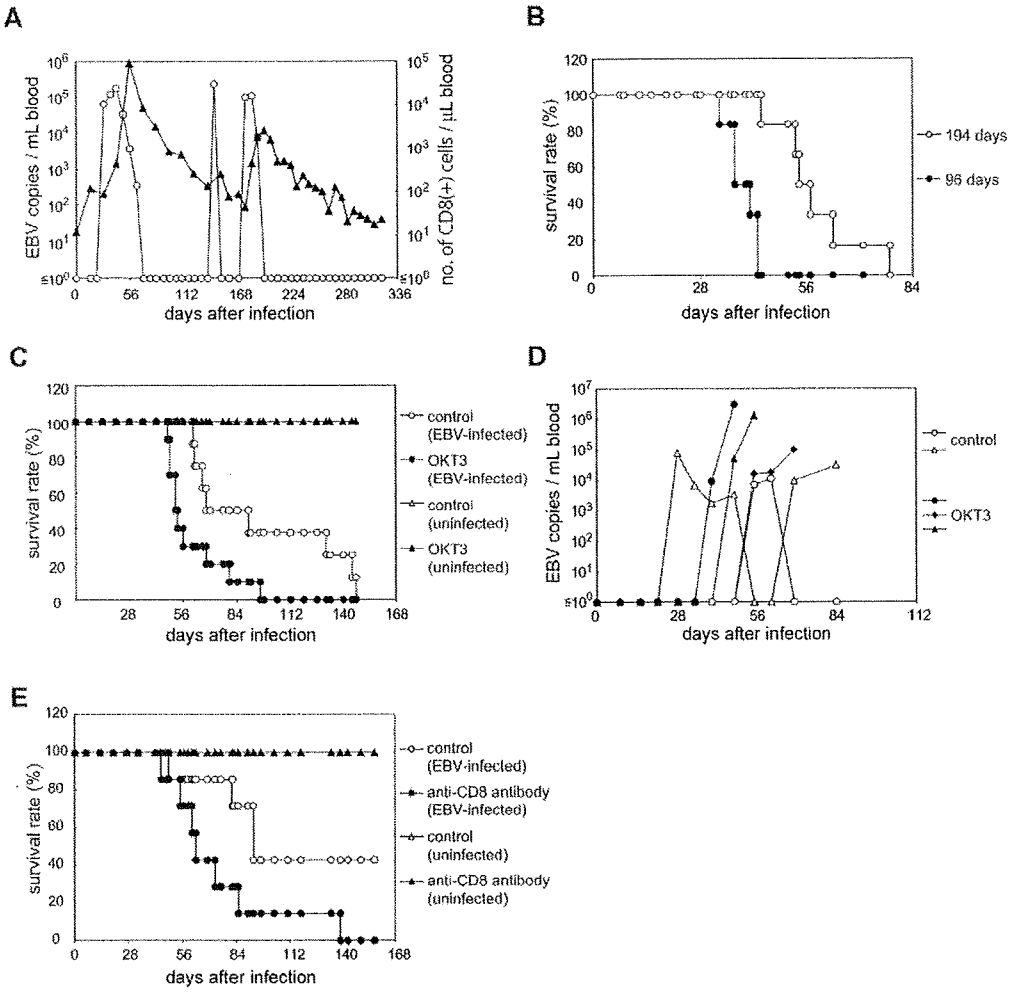

Figure 1. Evidence for T cell–mediated control of Epstein-Barr virus (EBV) infection in humanized NOD/Shi-*scid*/interleukin-2Rγ^{null} (NOG) mice. *A,* Associated changes in the number of CD8$^+$ T cells and viral DNA level in the peripheral blood of an EBV-infected humanized NOG mouse inoculated with EBV at ten 50% transformation dose (TD_{50}). The levels of EBV DNA *(open circles)* and CD8$^+$ T cells *(black triangles)* were monitored periodically. *B,* Survival curves of humanized NOG mice inoculated with EBV at different stages of reconstitution with human lymphocytes. Black circles represent mice inoculated with EBV (1×10^3 TD_{50}) at 96 days after transplantation with hematopoietic stem cells, and open circles represent mice inoculated at 194 days. *C,* Effect of depletion of T cells on the survival of EBV-infected humanized NOG mice. Black circles represent mice given daily intravenous injection with the OKT3 antibody (2 μg/mouse/day), starting at 21 days after infection, and open circles represent mice not given the antibody. Black triangles represent EBV-uninfected humanized NOG mice given OKT3 antibody, and open triangles represent such mice not given the antibody. *D,* Effect of depletion of T cells on the peripheral blood level of EBV DNA in humanized NOG mice. Black circles, black triangles, and black diamonds represent 3 humanized NOG mice inoculated with EBV (1×10^3 TD_{50}) that were treated with OKT3 as described in *C,* and open circles and open triangles represent such mice not treated with the antibody. Interruption of records indicates the death of a mouse. *E,* Effect of antibody specific to the CD8 molecule (B9.11) on the survival of EBV-infected humanized NOG mice. Black circles represent EBV-infected humanized NOG mice given daily intravenous injection with B9.11 (2 μg/mouse/day), starting at 21 days after infection, and open circles represent such mice not given the injection. Black triangles represent humanized NOG mice not infected with EBV that were given OKT3 antibody, and open triangles represent such mice not given the antibody.

stitutional Review Boards of the National Research Institute for Child Health and Development, the National Institute of Infectious Diseases, and the Tokyo Cord Blood Bank.

Preparation of EBV inocula and their titration, intravenous inoculation to humanized NOG mice, and quantification of viral DNA were performed as described elsewhere [6]. In brief, virus production from Akata cells was stimulated by treatment with anti-IgG antibody (DAKO), and culture fluid was used as inoculum after filtration through a 0.45-μm membrane filter. EBV titers in TD_{50} were determined by the Reed-Muench method.

In T cell reduction experiments, humanized NOG mice were inoculated with EBV at a dose of 1×10^2 TD_{50}. Starting at 21 days after inoculation, the Orthoclone OKT3 antibody specific to CD3 (Janssen Pharmaceutical) or the B9.11 antibody specific to CD8 (Beckman-Coulter) was administered intravenously at a dosage of 2 μg/mouse/day everyday until the end of the experiment. In a typical mouse treated with OKT3, 0.1% of human $CD45^+$ cells were $CD4^+CD8^-$ and 0.8% were $CD4^-CD8^+$ 2 weeks after the initiation of OKT3 administration, whereas in a control mouse, 15.0% of human $CD45^+$ cells were $CD4^+CD8^-$ and 12.5% were $CD4^-CD8^+$. Thus, this antibody was effective in significantly reducing the number of specific target cells. Confirmation of the reduction of $CD8^+$ cells by B9.11 was not possible, because this antibody covered the epitope recognized by antibodies available for flow cytometry. Survival curves of antibody-treated and untreated mice were compared statistically by the log-rank test.

Direct suppression of EBV-induced B cell transformation by $CD8^+$ T cells was assessed by the transformation regression assay based on a previously described method [11, 12]. $CD8^+$ T cells were isolated, as described elsewhere [6], from the spleen of EBV-infected or uninfected humanized NOG mice. Mononuclear cells were isolated from the spleen of uninfected humanized NOG mice and were inoculated with EBV (3×10^3 TD_{50} per 1×10^7 splenocytes). These EBV-infected cells were dispensed into microplates (3×10^4–1×10^5 cells/well) and were mixed with $CD8^+$ T cells.in the wells of microculture plates at different ratios. Half of the medium was replaced with fresh medium each week, and the outgrowth of lymphoblastoid cell lines was counted 8 weeks after initiation of the culture. Humanized NOG mice in the same lot were used in each experiment to attain common background of human major histocompatibility complex. The number of $CD8^+$ T cells required to achieve regression in 50% of the wells (50% regression dose) was calculated by the Reed-Muench method.

Results. Our previous experiments indicated that EBV-infected humanized NOG mice mount an EBV-specific T cell response that may be involved in immunological control of EBV. A time course of the levels of EBV DNA and $CD8^+$ T cells in the peripheral blood of a representative EBV-infected mouse (Figure 1*A*) suggested that these parameters change in an associated manner; there was a tendency for $CD8^+$ T cells to increase after surges in the EBV DNA level and to gradually decrease as the EBV DNA level decreased, suggesting that these $CD8^+$ T cells have some role in the control of EBV DNA level.

Table 1. Fifty Percent Regression Dose of $CD8^+$ T Cells in Epstein-Barr Virus (EBV)–Infected and Uninfected Mice

	50% Regression dose	
Experiment[a]	EBV-infected mice	Uninfected mice
A1	2.7×10^4	$>9.9 \times 10^4$
B1-1	2.7×10^5	$>1.4 \times 10^6$
B1-2	2.4×10^5	$>8.5 \times 10^5$
B2	1.1×10^5	$>4.2 \times 10^5$
B3[b]	$>2.3 \times 10^5$	$>3.0 \times 10^5$
C1[b]	$>3.9 \times 10^5$	$>3.2 \times 10^5$
C2	2.0×10^4	$>1.7 \times 10^5$

[a] Alphabetical letters signify the lot of a mouse, and the number immediately after the letter indicates an individual mouse. Numbers after a hyphen identify individual experiments.

[b] No significant regression was seen in these experiments.

To examine the protective role of T cells more precisely, we next tested whether the development of T cells has any influence on the mice's resistance to EBV infection. After transplantation with human HSCs, B cells develop first, ~3 months after transplantation, and T cells differentiate later, ~6 months after transplantation [10]. We divided 12 humanized NOG mice in a lot into 2 groups; 6 mice were inoculated with EBV (1×10^3 TD_{50}) at 96 days after transplantation with HSCs, and the remaining 6 were inoculated at 194 days. Mice were examined daily, and those exhibiting signs of severe illness, including weight loss, piloerection, and cachexia, were sacrificed for analysis. On autopsy, most of these mice showed the signs of lymphoproliferative disorder, as described elsewhere [6]. Figure 1*B* shows the survival curve of each group of infected mice, and the log-rank test indicated that the mice inoculated at 6 months after transplantation (ie, with fully developed T cells) had a significantly elongated life span ($P < .001$).

Because the aforementioned results suggested that T lymphocytes reconstituted in humanized NOG mice have some role in the protection against EBV-induced lymphoproliferative disorder, we then examined the effect of the anti-CD3 monoclonal antibody OKT3, which can deplete T cells in vivo [13]. Eighteen humanized NOG mice inoculated with 1×10^2 TD_{50} EBV were divided into 2 groups; 10 mice were given OKT3 beginning at 21 days after inoculation, and the remaining 8 were not given the antibody. Figure 1*C* shows the survival curve of these mice. The log-rank test indicated that those mice treated with OKT3 antibody had a significantly shorter life span, compared with control mice ($P < .01$). Similar OKT3 treatment

was performed with 7 humanized NOG mice that were not infected with EBV; 4 mice were given OKT3 antibody, and 3 were not. The result indicated that all mice in both groups survived the observation period of 150 days, and no difference could be seen between them, excluding the possibility that OKT3 has its own toxicity (Figure 1*C*). In accordance with this result, quantification with real-time polymerase chain reaction indicated that the level of EBV DNA in the peripheral blood was consistently higher in the OKT3-treated mice than in control mice (Figure 1*D*). Because $CD8^+$ cytotoxic T cells are considered to play a central role in the immune response to EBV, we next examined the effect of an antibody (B9.11) specific to the CD8 molecule [14]. Figure 1*E* shows the survival curves of EBV-infected humanized NOG mice that were either treated with B9.11 or not, and the log-rank test indicated that those mice treated with the antibody had a significantly reduced life span after EBV infection ($P < .05$).

To test whether T cells isolated from EBV-infected mice have the ability to suppress transformation of autologous B cells by EBV, we used the transformation regression assay. Mononuclear cells isolated from the spleen of humanized NOG mice were inoculated with EBV and were cocultured with $CD8^+$ T cells isolated from the spleen of either EBV-infected or uninfected mice. Table 1 shows the number of $CD8^+$ T cells required to inhibit the outgrowth of EBV-infected cells in 50% of the wells (50% regression dose). These data indicate that $CD8^+$ T cells isolated from EBV-infected mice, but not those from uninfected mice, could suppress the outgrowth of transformed lymphoblastoid cell line.

Discussion. Humanized mouse technology has been successfully used to reproduce human immune responses to certain viruses that cannot infect ordinary mice [6–8, 10]. However, these studies have yet to provide evidence that immune responses induced in these mice are actually involved in the control of viral infections. This was an important issue when we considered the possibility of using humanized mice as a tool to evaluate immunological therapies and prophylaxes to viral infections.

Humanized NOG mice in later stages of reconstitution that contained high numbers of T cells had significantly longer life spans after EBV infection, compared with those in earlier stages that lacked significant differentiation of T cells. In accordance with this result, treatment of EBV-infected humanized NOG mice with OKT3, which can deplete $CD3^+$ T cells, significantly reduced their life span. Furthermore, similar antibody-mediated reduction in the number of $CD8^+$ T cells also reduced the life span of infected humanized NOG mice. Thus, our results strongly suggest that human T cells that develop in humanized NOG mice contribute to their resistance to EBV infection. More-direct evidence of immunological control of EBV infection was obtained by the transformation regression assay, which has been used as one of the most reliable methods to quantify EBV-specific cytotoxic T cells. This assay clearly indicated that $CD8^+$ T cells isolated from EBV-infected mice can suppress EBV-induced transformation of autologous B cells. A study is underway to identify an epitope that can be recognized by a $CD8^+$ T cell clone.

To our knowledge, these results are the first evidence that immune responses induced in humanized mice are actually involved in an effective control of viral infection. It is thus suggested that the NOG mouse model of EBV infection is a useful tool to evaluate candidate vaccines and immunological therapies for EBV infection.

After the initial submission of this report, Strowig and others published a work containing similar findings, namely higher EBV load and lymphoproliferative disorder in humanized mice after T cell depletion [15].

Acknowledgments

We thank Motohiko Okano, for advice in regression assay; Miki Mizukami, Ken Watanabe, and Miki Katayama, for technical assistance; Yuko Tatsumi and Tomomi Hakuya, for secretarial assistance; and Tokyo Cord Blood Bank, for supplying cord blood.

References

1. Rickinson AB, Kieff E. Epstein-Barr virus. In: Knipe DM, Howley PM, eds. Fields virology. 5th ed. Vol. 2. Philadelphia: Lippincott Williams & Wilkins, **2007**:2655–700.
2. Kieff E, Rickinson AB. Epstein-Barr virus and its replication. In: Knipe DM, ed. Fields virology. 5th. ed. Vol. 2. Philadelphia: Lippincott Williams & Wilkins, **2007**:2603–54.
3. Hislop AD, Taylor GS, Sauce D, Rickinson AB. Cellular responses to viral infection in humans: lessons from Epstein-Barr virus. Annu Rev Immunol **2007**; 25:587–617.
4. Babcock GJ, Decker LL, Volk M, Thorley-Lawson DA. EBV persistence in memory B cells in vivo. Immunity **1998**; 9:395–404.
5. Ito M, Hiramatsu H, Kobayashi K, et al. NOD/SCID/gamma(c)(null) mouse: an excellent recipient mouse model for engraftment of human cells. Blood **2002**; 100:3175–82.
6. Yajima M, Imadome KI, Nakagawa A, et al. A new humanized mouse model of Epstein-Barr virus infection that reproduces persistent infection, lymphoproliferative disorder, and cell-mediated and humoral immune responses. J Infect Dis **2008**; 198:673–82.
7. Melkus MW, Estes JD, Padgett-Thomas A, et al. Humanized mice mount specific adaptive and innate immune responses to EBV and TSST-1. Nat Med **2006**; 12:1316–22.
8. Traggiai E, Chicha L, Mazzucchelli L, et al. Development of a human adaptive immune system in cord blood cell-transplanted mice. Science **2004**; 304:104–7.
9. Watanabe S, Ohta S, Yajima M, et al. Humanized NOD/SCID/IL2Rgamma(null) mice transplanted with hematopoietic stem cells under nonmyeloablative condition show prolonged lifespans and allow detailed analysis of human immunodeficiency virus type 1 pathogenesis. J Virol **2007**; 81:13259–64.
10. Watanabe S, Terashima K, Ohta S, et al. Hematopoietic stem cell-engrafted NOD/SCID/IL2Rgamma null mice develop human lymphoid

systems and induce long-lasting HIV-1 infection with specific humoral immune responses. Blood **2007**; 109:212–8.
11. Moss DJ, Rickinson AB, Pope JH. Long-term T-cell-mediated immunity to Epstein-Barr virus in man. I. Complete regression of virus-induced transformation in cultures of seropositive donor leukocytes. Int J Cancer **1978**; 22:662–8.
12. Okano M, Purtilo DT. Simple assay for evaluation of Epstein-Barr virus specific cytotoxic T lymphocytes. J Immunol Methods **1995**; 184:149–52.
13. Dessureault S, Shpitz B, Alloo J, et al. Physiologic human T-cell responses to OKT3 in the human peripheral blood lymphocyte-severe combined immunodeficiency mouse model. Transplantation **1997**; 64: 811–6.
14. Kobayashi E, Kawai K, Ikarashi Y, Fujiwara M. Mechanism of the rejection of major histocompatibility complex class I-disparate murine skin grafts: rejection can be mediated by CD4+ cells activated by allo-class I + II antigen in CD8+ cell-depleted hosts. J Exp Med **1992**; 176: 617–21.
15. Strowig T, Gurer C, Ploss A, et al. Priming of protective T cell responses against virus-induced tumors in mice with human immune system components. J Exp Med **2009**; 206:1423–34.

Epstein–Barr virus-encoded latent membrane protein 1 activates β-catenin signaling in B lymphocytes

Mariko Tomita,[1] Md. Zahidunnabi Dewan,[2,3,5] Naoki Yamamoto,[2,3] Akira Kikuchi[4] and Naoki Mori[1,6]

[1]Division of Molecular Virology and Oncology, Graduate School of Medicine, University of the Ryukyus, Okinawa; [2]Department of Molecular Virology, Graduate School, Tokyo Medical and Dental University, Tokyo; [3]AIDS Research Center, National Institute of Infectious Disease, Tokyo; [4]Department of Biochemistry, Graduate School of Biomedical Science, Hiroshima University, Hiroshima, Japan

(Received November 28, 2008/Revised January 4, 2009/Accepted January 21, 2009/Online publication March 20, 2009)

The Epstein–Barr virus-encoded latent membrane protein 1 is considered the Epstein–Barr virus oncogene based on its importance in Epstein–Barr virus-induced B-lymphocyte transformation. β-Catenin is a potential oncogene, and its accumulation has been implicated in a variety of human cancers. Here, we found that β-catenin protein was highly expressed in Epstein–Barr virus-immortalized B-cell lines compared with peripheral blood mononuclear cells from healthy donors. β-Catenin expression in Epstein–Barr virus-immortalized B-cell line decreased following treatment with LY294002, an inhibitor of phosphatidylinositol 3-kinase. Treatment with LY294002 or knockdown of β-catenin by small interfering RNA reduced the growth of Epstein–Barr virus-immortalized B-cell line. Transient transfection of latent membrane protein 1 expression plasmid increased β-catenin protein expression and β-catenin-dependent transcription. Latent membrane protein 1 deletions mutants lacking the carboxyl-terminal activating region 1 domain failed to enhance β-catenin protein expression and β-catenin-dependent transcriptional activity. They also failed to increase phosphorylated AKT expression. Dominant-negative AKT suppressed latent membrane protein 1-induced β-catenin-dependent transcriptional activity. These results suggest that latent membrane protein 1 activates β-catenin through the phosphatidylinositol 3-kinase/AKT signaling pathway. Activation of the β-catenin pathway by Epstein–Barr virus may contribute to the lymphoproliferation characteristic of Epstein–Barr virus-infected B-cells. (*Cancer Sci* 2009; 100: 807–812)

Epstein–Barr virus (EBV), a member of the herpes virus family, has been identified as the first human tumor virus associated with several malignancies. Cancers linked to EBV include lymphomas that develop in the immunocompromised individuals, Hodgkin's disease, Burkitt's lymphoma, and nasopharyngeal carcinoma.[1] Regardless of their type, the majority of tumor cells are latently infected with EBV. LMP1, a viral latency protein, is considered an EBV oncogene based on its importance in EBV-induced B-lymphocyte transformation.[2] LMP1 is an integral membrane protein consisting of 386 amino acids that form a short amino-terminal cytoplasmic end, six hydrophobic transmembrane domains, and a long carboxyl-terminal tail that contains the two main signaling domains, CTAR-1 and -2.[3] Through self clustering in the membrane, LMP1 acts as a constitutively active TNF receptor and mimics many of the phenotypic consequences of TNF receptor family such as TNF receptor and CD40 activation. CTAR-1 interacts with members of the TRAF family, TRAF1 and TRAF2, and induces NF-κB signaling.[4,5] CTAR-2 associates with TRADD protein and also mediates NF-κB signaling.[6] CTAR-2 also induces the activity of AP-1 transcription factor via signaling pathway that involves c-Jun N-terminal kinase.[7,8] LMP1 also activates p38 MAPK through both CTAR-1 and CTAR-2.[9] In addition, LMP1 activates the p44/p42 MAPK[10] and JAK/STAT[11] pathways.

Phosphatidylinositol 3-kinase (PI3K)/AKT signaling is often activated in many human cancer cells.[12] It is activated by a wide range of extracellular growth and mitogenic stimuli including ligands of the TNF receptor family, thus suggesting that LMP1 may also target this pathway. Indeed, previous studies have shown that LMP1 can activate the PI3K/AKT pathway.[13,14] CTAR-1 activates PI3K/AKT signaling, resulting in the phosphorylation of the AKT target, GSK3β. The activation of PI3K/AKT is responsible for LMP1-induced actin polymerization and transformation, and also contributes to cell survival.[13,14]

The Wnt/β-catenin signaling cascade is an important pathway activated in various cancers. β-Catenin is a critical component of the Wnt signaling pathway.[15] Stabilized or free β-catenin can translocate to the nucleus and bind transcription factors, such as the Tcf or Lef, to activate transcription. β-Catenin-Tcf/Lef complexes regulate a number of protooncogenes, including *c-myc* and *cyclin D1*. Previous studies have shown that β-catenin is a potential oncogene,[16] and its accumulation has been implicated in a variety of human cancer cells.[17]

We reported previously that HTLV-1, the causative agent of ATL, induces β-catenin protein accumulation and transcriptional activation via the PI3K/AKT signaling pathway.[18] LMP1 also activates PI3K/AKT pathway;[13,14] however, the role of LMP1 in β-catenin regulation through this signaling pathway in B lymphocytes has not yet been established. In this study, we determined whether the LMP1-mediated effects on PI3K/AKT signaling modulated β-catenin expression in EBV-infected B cells.

Materials and Methods

Reagents. PI3K inhibitor LY294002 and the MEK1/2 inhibitor PD98059 were purchased from Calbiochem (La Jolla, CA, USA).

Antibodies. We used primary antibodies against β-catenin (BD Transduction Laboratories, San Jose, CA, USA), LMP1 (CS.1–4) (Dako, Glostrup, Denmark), actin (Lab Vision, Fremont, CA, USA), phospho-AKT (Ser473), AKT, phospho-p44/p42 MAPK (Erk1/2) (Thr202/Tyr204), and p44/p42 MAPK (Erk1/2) (Cell Signaling Technology, Beverly, MA, USA). Horseradish-peroxidase-conjugated secondary antibodies were purchased from GE Healthcare (Waukesha, WI, USA).

Cell lines. EBV-immortalized LCLs (LCL-Ao, LCL-Ka, and LCL-Ku) were established by infection of lymphocytes from three healthy donors with culture supernatants of the virus producer

[5]Present address: Department of Pathology, New York University School of Medicine, New York, USA.
[6]To whom correspondence should be addressed. E-mail: n-mori@med.u-ryukyu.ac.jp

Abbreviations: ATL, adult T-cell leukemia; CTAR, carboxyl-terminal activating region; EBV, Epstein-Barr virus; GSK3β, glycogen synthase kinase 3β; HTLV-1, human T-cell leukemia virus type 1; JAK/STAT, janus kinase/signal transducers and activators of transcription; LCLs, lymphoblastoid cell lines; Lef, lymphocyte enhancer factor; LMP, latent membrane protein; MAPK, mitogen-activated protein kinase; MEK1/2, mitogen-activated protein/extracellular signal-regulated kinase; MTT, 3-(4,5-Dimethyl-2-thiazolyl)-2,5-diphenyl-*2H*-tetrazolium bromide; NF-κB, nuclear factor-kappaB; PI3K, phosphatidylinositol 3-kinase; PBMC, peripheral blood mononuclear cells; SDS-PAGE, sodium dodecyl sulfate–polyacrylamide gel electrophoresis; siRNA, small interfering RNA; Tcf, T-cell factor; TK, tymidine kinase; TNF, tumor necrosis factor; TRADD, TNF receptor-associated death domain protein; TRAF, TNF receptor-associated factor; WST-8, 2-(2-methoxy-4-nitrophenyl)-3(4-nitrophenyl)-5-(2,4-disulfophenyl)-*2h* tetrazolium monosodium salt.

doi: 10.1111/j.1349-7006.2009.01121.x

B95.8 line as described previously,[19] and cultured in RPMI-1640 medium supplemented with 10% heat-inactivated fetal bovine serum, 50 U/mL penicillin, and 50 μg/mL streptomycin at 37°C in 5% CO_2. HeLa cells (human cervix adenocarcinoma cell line) were maintained in Dulbecco's modified Eagle's medium supplemented with 10% heat-inactivated fetal bovine serum, 50 U/mL penicillin, and 50 μg/mL streptomycin at 37°C in 5% CO_2.

Peripheral blood mononuclear cells (PBMCs). PBMCs from healthy volunteers were isolated by Ficoll-Paque density gradient centrifugation (GE Healthcare). All blood samples were obtained after informed consent.

Western blot analysis. Western blot analysis was performed as described previously.[20] In brief, whole cell lysates were subjected to SDS-PAGE, electroblotted onto polyvinylidene difluoride membranes (Millipore, Billerica, MA, USA) and then analyzed for immunoreactivity with the appropriate primary and secondary antibodies as indicated in the figures. Reaction products were visualized using Enhanced Chemiluminescence reagent, according to the instructions provided by the manufacturer (Amersham Pharmacia, Uppsala, Sweden).

Cellular proliferation assay. Proliferation of LCL-Ka cells after treatment with LY294002 or PD98059 was analyzed by counting viable cells using the Trypan blue exclusion method. The antiproliferative effects of LY294002 against LCL-Ka and PBMCs from a healthy donor were measured by the WST-8 method (Cell Counting Kit-8; Wako Pure Chemical Industries, Osaka, Japan) based on the MTT assay, as described previously.[21] Briefly, the 5×10^3 cells were incubated in triplicate in a 96-well microculture plate in the presence of different concentrations of LY294002 (0–50 μM) in a final volume of 0.1 mL for 48 h at 37°C. Thereafter, 5-μL Cell Counting Kit-8 solution (5 mM WST-8, 0.2 mM 1-methoxy 5-methylphenazinium methylsulfate, and 150 mM NaCl) was added, and the cells were further incubated for another 4 h. The number of surviving cells was measured by a 96-well multiscanner autoreader at optical density of 450 nm. Cell viability was determined as percentage of the control (absence of LY294002).

Small interfering RNA (siRNA). To repress β-catenin, a predesigned double-stranded siRNA (siGENOME SMARTpool CTNNB1; Dharmacon, Lafayette, CO, USA) was used. A siCONTROL nontargeting siRNA pool (Dharmacon) was used as a negative control. siRNA was transfected into LCL-Ka cells at 100 nM of the final concentration. The transfected cells were incubated for 12 h, seeded into 24-well plates at 5×10^4 viable cells per well, and incubated for the indicated time periods. The number of viable cells was determined every 24 h by counting Trypan blue excluding cells in a hemocytometer.

Plasmids. The β-catenin expression plasmid (pCGN/β-catenin) and human Tcf-4 expression plasmid (pEF-BOS HA/Tcf-4E) have been described previously.[22,23] The pGL3-OT and pGL3-OF reporter plasmids[24] were kindly provided by Dr B. Vogelstein (Sidney Kimmel Comprehensive Cancer Center, Johns Hopkins University School of Medicine, Baltimore, MD, USA). pGL3-OT and pGL3-OF contain three copies of the Tcf site (5′-AGATCAA AGG-3′) and a mutant sequence (5′-AGGCCAAAGG-3′), respectively, upstream of the c-*fos* promoter and the luciferase open reading frame. The expression plasmids pSG5-LMP1, pSG5-LMP1Δ187-351, pSG5-LMP1349Δ, and pSG5-LMP1Δ194-386 were provided by Dr M. Rowe (University of Wales College of Medicine, Cardiff, UK).[25,26] The dominant-negative AKT expression plasmid (pCMV5-K169A, T308A, S473A-AKT) had Lys-169-, Thr-308-, and Ser-473-to-Ala mutations and was kindly provided by Dr D. Alessi (University of Dundee, Dundee, UK).

Transfection. HeLa cells were transfected using Lipofectamine reagent (Invitrogen, Carlsbad, CA, USA) according to the protocol supplied by the manufacturer. LCL-Ka cells were transfected by using MicroPorator MP-100 (Digital Bio Technology, Seoul, Korea) according to the instructions supplied by the manufacturer for optimization and use.

Luciferase assay. Cells were transiently transfected with the indicated effecter plasmids and a luciferase reporter construct. In all cases, the reference plasmid phRL-TK (Promega, Madison, WI, USA), which contains the *Renilla* luciferase gene under the control of the TK promoter, was cotransfected to correct for transfection efficiency. Luciferase assays were performed by using the Dual-Luciferase Reporter System (Promega), in which relative luciferase activities were calculated by normalizing transfection efficiency according to the *Renilla* luciferase activities.

Statistical analysis. Data of cell proliferation assay were expressed as mean ± SD. Differences between groups were examined for statistical significance by the unpaired Student's *t*-test. A *P*-value less than 0.05 denoted the presence of a statistically significant difference.

Results

β-Catenin protein is highly expressed in EBV-immortalized B-cells and correlates with LMP1 expression and AKT phosphorylation. First, we analyzed protein expression of β-catenin in EBV-immortalized B-cell lines. β-Catenin protein was highly expressed in EBV-immortalized B-cell lines compared with normal PBMCs (Fig. 1a). Although the expression of β-catenin was higher in LCLs than in normal PBMCs, β-catenin expression level varied among EBV-immortalized B-cell lines (highest expression in LCL-Ka and lowest expression in LCL-Ao). To determine whether AKT activity is associated with β-catenin expression in EBV-infected cells, we examined the phosphorylation status of AKT relative to β-catenin protein expression in EBV-immortalized B-cell lines (Fig. 1a). Phosphorylated AKT and β-catenin were detected in all EBV-immortalized B-cell lines, and the expression levels of these proteins were similar to those of LMP1 in these cells.

PI3K/AKT signaling contributes to β-catenin expression and EBV-immortalized B-cell growth. Next, to determine the role of PI3K/AKT signaling in the expression of β-catenin in EBV-immortalized B-cell lines, LCL-Ka cells, which expressed the highest levels of β-catenin, LMP1, and phosphorylated AKT proteins among EBV-immortalized B-cell lines, were treated with the PI3K inhibitor LY294002 (Fig. 1b). β-Catenin expression was significantly reduced in the presence of LY294002. Phosphorylation of AKT was also inhibited by LY290042, whereas the total level of AKT was unaffected. Treatment with LY294002 did not change the expression of LMP1. On the other hand, MEK1/2 inhibitor PD98059 did not change both β-catenin and phosphorylated AKT protein levels, although it decreased the level of phosphorylated p44/p42 MAPK.

To elucidate the effect of PI3K/AKT signaling on the growth of EBV-immortalized B cells, LCL-Ka cells were first treated with either PD98059 or LY294002, followed by counting the cell numbers at 1, 2, and 3 days (Fig. 1c, left panel). The growth of LCL-Ka cells were suppressed by both PD98059 and LY294002 treatments. However, the effect of LY294002 was greater than that of PD98059. To verify the specificity of LY294002 and rule out nonspecific toxicity of this drug, we also analyzed the effect of LY294002 on the viability of PBMCs from a healthy donor, whose PI3K/AKT signaling pathway was not activated. The result of these analyses demonstrated that inhibition of PI3K/AKT signaling pathway by LY294002 did not suppress cell viability of PBMCs from a healthy donor (Fig. 1c, right panel), indicating that the effects of LY294002 on LCL-Ka were not non-specific toxicity of this drug. We also found that knockdown of β-catenin by siRNA inhibited the growth of LCL-Ka cells (Fig. 1d, left panel). The efficiency of knockdown was moderate (Fig. 1d, right panel) due to the low transfection efficiency (40–50%) of these cells (data not shown).

LMP1 induces expression and transcriptional responses of β-catenin. Next, we examined the role of LMP1 in the expression of β-catenin. β-Catenin protein expression was induced by transient transfection of LMP1 expression plasmids (Fig. 2a). We next examined whether the induction of β-catenin by LMP1 affected

doi: 10.1111/j.1349-7006.2009.01121.x

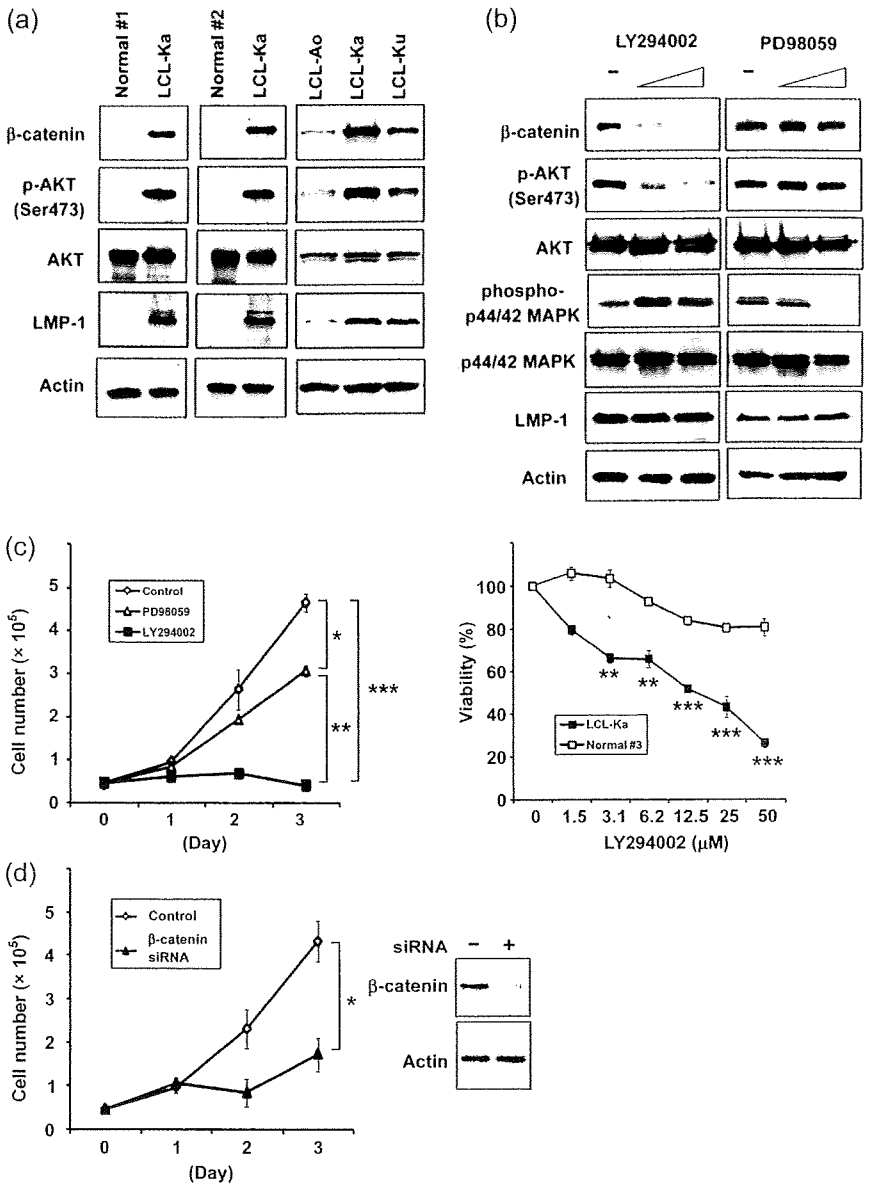

Fig. 1. Inhibition of phosphatidylinositol 3-kinase (PI3K)/AKT reduced β-catenin expression and cell growth of Epstein–Barr vius (EBV)-immortalized B-cell lines. (a) Total cell lysates of EBV-immortalized B-cell lines (lymphoblastoid cel lines [LCL]-Ao, LCL-Ka, and LCL-Ku) and normal peripheral blood mononuclear cells (PBMCs) (Normal #1 and #2) were resolved in sodium dodecyl sulfate–polyacrylamide gel electrophoresis (SDS-PAGE) and probed with anti-β-catenin, antiphospho-AKT (Ser473), anti-AKT, and anti-latent membrane protein 1 (LMP1) antibodies. Actin was the loading control. (b) LCL-Ka cells were treated with increasing amounts (0, 25, and 50 μM) of PI3K inhibitor LY294002 or mitogen-activated protein/extracellular signal-regulated kinase inhibitor PD98059 for 48 h. Total cell lysates were resolved in SDS-PAGE and probed with anti-β-catenin, antiphospho-AKT (Ser473), anti-AKT, antiphospho p44/p42 mitogen-activated protein kinase (MAPK), antip44/p42 MAPK, and anti-LMP1 antibodies. Actin was the loading control. Representative results of three experiments with similar findings. (c) PI3K inhibitor LY294002 suppressed the growth of EBV-immortalized B-cell line. LCL-Ka cells (5×10^4 cells/mL) were treated with 50 μM of either LY294002 or PD98059, or vehicle (control) for the indicated time periods. Viable cell numbers were counted in triplicate by Trypan blue dye exclusion method. Data are mean ± SD of three separate experiments ($^*P < 0.01$, $^{**}P < 0.001$ and $^{***}P < 0.0005$) (left panel). LCL-Ka cells and PBMCs from a healthy donor (Normal #3) were treated with increasing amount of LY294002 (0–50 μM) for 48 h. Cell viability was assessed by the 2-(2-methoxy-4-nitrophenyl)-3(4-nitrophenyl)-5-(2,4-disulfophenyl)-*2h* tetrazolium monosodium salt (WST-8) method. Data are expressed as the mean ± SD percentage of the control (untreated cells). Significance of differences between percentage viable cells of LY294002 treated cells and that of untreated cells are shown as *P*-values ($^{**}P < 0.001$ and $^{***}P < 0.0005$) (right panel). (d) Knockdown of β-catenin suppressed the growth of EBV-immortalized B-cell line. LCL-Ka cells were transfected with siRNA for β-catenin or with a non-target siRNA (final concentration of siRNA was 100 nM). The effect of knockdown of β-catenin on cell growth was examined by counting the number of viable cells in triplicate using the trypan blue dye-exclusion method (left panel). Data are mean ± SD of three separate experiments ($^*P < 0.05$). Western blotting analysis showing repression of β-catenin in LCL-Ka cells transfected with β-catenin siRNA (+) compared with that in cells transfected with non-targeting siRNA (–) (right panel). Cells were collected 48 h after transfection. Actin was the loading control. Representative results of three experiments with similar findings.

β-catenin/Tcf transcriptional activity (Fig. 2b). In a transient transfection reporter assay using pGL3-OT as a reporter, the expression of LMP1 alone in HeLa cells activated the reporter activity. The combination of β-catenin and LMP1 had an even greater effect. No significant responses were seen with the mutant reporter (pGL3-OF) (data not shown).

CTAR-1 is required for activation of β-catenin by LMP1. To identify the domain within the LMP1 cytoplasmic tail responsible for the induction of the transcriptional activity of β-catenin/Tcf, reporter assay was performed with LMP1 mutants defective for the CTAR-1 and CTAR-2 effecter domains (Fig. 3b). Figure 3(a) (left panel) shows schematic diagrams of the wild type and mutants of LMP1 expression plasmids. HeLa cells transfected with either the wild-type or mutants LMP1 expression plasmids expressed comparable levels of LMP1 protein as determined by western blotting (Fig. 3a, right panel). The LMP1 CTAR-1/CTAR-2 double mutant Δ194-386 was not detected by CS. 1–4 antibodies since it lacks the epitopes recognized by these antibodies. Expression of the CTAR-1 mutant Δ187-351 showed little induction of reporter activation, implicating CTAR-1 as the domain of LMP1 responsible for this response. This was confirmed with the CTAR-2 mutant 349Δ, where the expression resulted in activation of the reporter, similar to the wild-type LMP1. The CTAR-1/CTAR-2 double mutant Δ194-386 failed to induce reporter activation, consistent with the role of CTAR-1 in this effect. Next, we analyzed the effect of CTAR-1 on the induction of β-catenin protein expression (Fig. 3c). Transient transfection of either the wild-type or mutant LMP1 expression plasmids in HeLa cells showed that CTAR-1 mutant Δ187-351 and CTAR-1/CTAR-2 double mutant Δ194-386 had little effects on the induction of β-catenin protein than wild-type and CTAR-2 mutant 349Δ.

Activation of β-catenin by LMP1 is associated with AKT activity. Activation of AKT signaling is associated with accumulation of β-catenin.[27] To determine whether AKT activation is associated

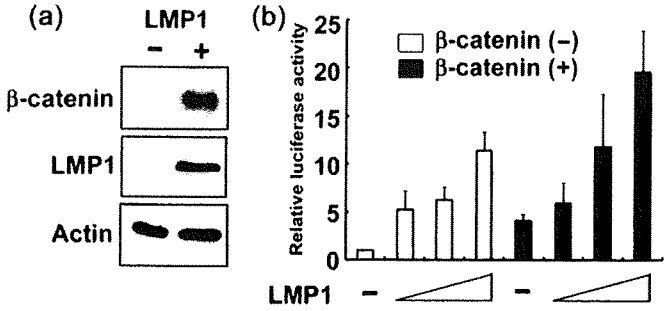

Fig. 2. Latent membrane protein 1 (LMP1) induced expression and transcriptional responses of β-catenin. (a) LMP1 induced expression of β-catenin protein. HeLa cells were transfected with either 2 μg of LMP1 expression plasmid (+) or empty vector (–). Cells were collected 48 h after transfection. Total cell extracts from transfected HeLa cells were analyzed for β-catenin and LMP1 protein expression by western blot analysis. Actin was a loading control. Representative results of three experiments with similar findings. (b) Transient expression assay evaluating the activity of β-catenin/T-cell factor (Tcf)-regulated reporter. HeLa cells were transfected with the pGL3-OT reporter (2 μg), Tcf (0.1 μg), and either LMP1 (0, 0.5, 1, or 2 μg) or β-catenin (0.5 μg) plus LMP1. Cells were collected 48 h after transfection. Data are mean ± SD of triplicate experiments.

with LMP1-induced β-catenin activity, we examined the phosphorylation status of AKT in HeLa cells transiently transfected with either wild-type or mutant LMP1 expression plasmids (Fig. 3c). CTAR-1 mutant Δ187-351 and CTAR-1/CTAR-2 double mutant Δ194-386 had less important effects on the phosphorylation of AKT than wild-type and CTAR-2 mutant 349Δ. These results indicate that LMP1 activates AKT through CTAR-1 cytoplasmic tail.

Dominant-negative AKT suppresses LMP1-induced β-catenin/Tcf transcriptional activity. To determine the role of AKT in the LMP1-induced β-catenin/Tcf transcriptional activity, we used the dominant-negative mutant AKT expression plasmid, AKT-DN, to directly examine the role of AKT in LMP1-induced β-catenin/Tcf transcription (Fig. 3d). AKT-DN suppressed the LMP1-induced pGL3-OT activity. pGL-OF activity was not affected by AKT-DN plasmid (data not shown).

Discussion

EBV-positive malignancies in immunocompromised patients are associated with high mortality and reduced overall survival period. Here, we demonstrated the important roles of β-catenin in the growth of EBV-immortalized B-cell lines and the role of LMP1 in activation of β-catenin in these cells. We found that EBV-immortalized B cell lines highly expressed β-catenin protein compared with normal PBMCs. Knockdown of β-catenin by siRNA reduced the growth of LCL-Ka cells, indicating that β-catenin plays an important role in the growth of EBV-immortalized B cell lines. EBV transforming protein LMP1 induced β-catenin protein expression and transcriptional activity. β-Catenin protein levels in LCL-Ka cells were reduced by treatment with PI3K inhibitor LY294002. In this regard, a recent study has shown that LMP1 regulates epithelial cell motility and invasion via the ERK/MAPK pathway.[28] We also found that MEK1/2 inhibitor, PD98059, suppressed the growth of LCL-Ka cells without decreasing β-catenin expression. However, the effect of PD98059 was less pronounced than that of LY294002, suggesting that β-catenin may have a dominant role in the growth of these cells. Moreover, dominant-negative AKT inhibited LMP1-induced β-catenin-dependent transcription. These results suggest that LMP1 activates β-catenin via the PI3K/AKT signaling pathway.

Previous studies reported that LMP1 activates PI3K/AKT signaling, resulting in enhancement of cell transformation and survival of epithelial cells.[13,14] Here, we showed that the same signaling

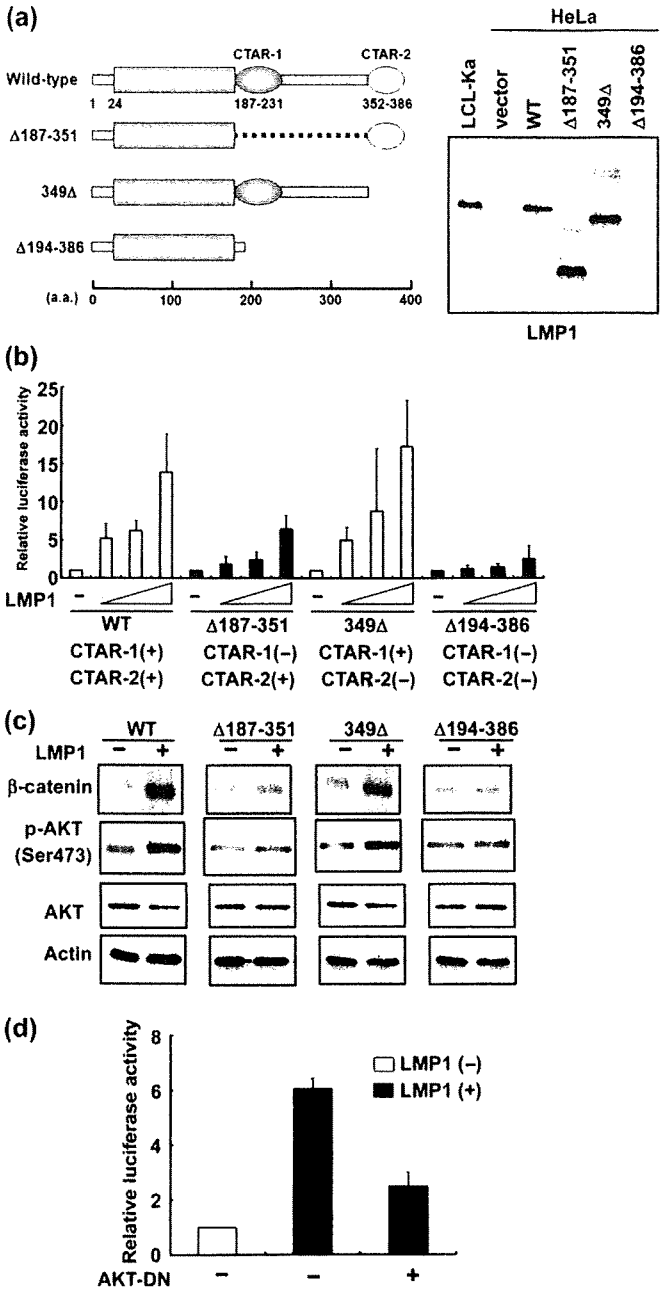

Fig. 3. Carboxyl-terminal activating region 1 (CTAR-1) is required for activation of β-catenin/T-cell factor (Tcf) transcription by latent membrane protein 1 (LMP1). (a) Schematic diagrams of wild-type (WT) and mutants LMP1 (left panel). HeLa cells were transfected with either wild-type or mutant LMP1 expression plasmids (right panel). Cells were collected 48 h after transfection and total lysates were analyzed for LMP1 expression by western blot analysis. (b) HeLa cells were transfected with the pGL3-OT reporter (2 μg), Tcf expression plasmid (0.1 μg), and either LMP1 wild-type or LMP1 mutants (Δ187-351, 349Δ, or Δ194-386) (0, 0.5, 1, or 2 μg). Cells were collected 48 h after transfection. Data are mean ± SD of triplicate experiments. (c) HeLa cells were transfected with either wild-type LMP1 or LMP1 mutants (Δ187-351, 349Δ, and Δ194-386) expression plasmids (2 μg). Cells were collected 48 h after transfection. Total cell extracts from transfected HeLa cells were analyzed for β-catenin expression levels and phosphorylation status of AKT by western blot analysis. Actin was a loading control. Representative results of three experiments with similar findings. (d) Dominant-negative AKT suppressed LMP1-induced β-catenin/Tcf transcription. HeLa cells were transfected with the pGL3-OT reporter (2 μg), Tcf (0.1 μg), and either LMP1 (0.5 μg) or LMP1 with dominant-negative AKT (AKT-DN) (0.1 μg) as indicated in the figure. Cells were collected 48 h after transfection. AKT-DN suppressed LMP1-induced β-catenin/Tcf transcription. Data are mean ± SD of triplicate experiments.

doi: 10.1111/j.1349-7006.2009.01121.x

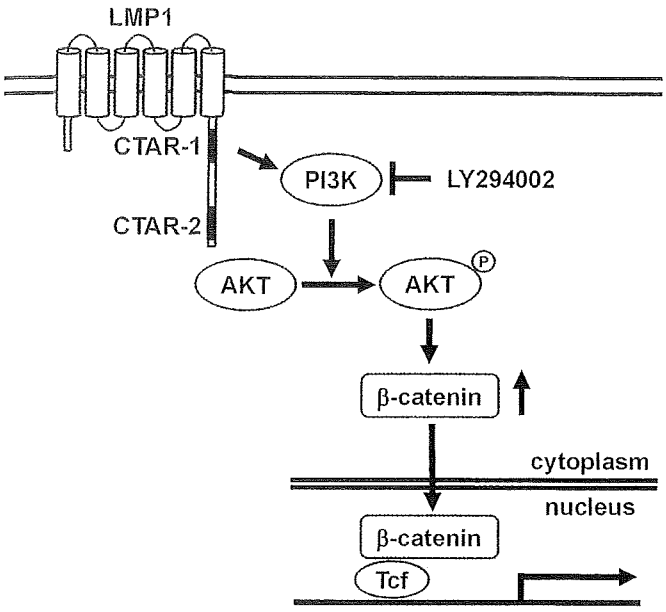

Fig. 4. Schematic representation of the effects of latent membrane protein 1 (LMP1) on the β-catenin signaling pathway. LMP1 activates phosphatidylinositol 3-kinase (PI3K)/AKT through carboxyl-terminal activating region 1 (CTAR-1) cytoplasmic tail. The activated AKT enhances β-catenin protein expression. Highly expressed β-catenin can translocate to the nucleus and bind to the transcription factor T-cell factor (Tcf).

is also important for the growth of EBV-immortalized B cells. They also demonstrated that the cytoplasmic COOH terminus of LMP1 is necessary for activation of PI3K/AKT signaling.[13] We confirmed these findings by showing that LMP1 mutants deficient in the CTAR-1 domain could not activate phosphorylation of AKT. LMP1 most closely resembles an activated CD40 in its phenotypic effects. In this regard, one study reported that CD40 ligation can activate PI3K/AKT signaling in B cells and that this effect is important for both cell proliferation and survival.[29] Furthermore, mice deficient in the p85 subunit of PI3K are severely impaired in B cell development with reduced proliferative responses to CD40 ligation.[30] Taken together, these data highlight the role of the PI3K/AKT signaling pathway in B cell growth and suggest that the ability of LMP1 to activate this pathway contributes to EBV persistence in B cells.

The Wnt/β-catenin signaling pathway has been identified as a common target for perturbation by viruses, as demonstrated by the following examples from the literature. HTLV-1 Tax, which activates PI3K/AKT signaling, results in GSK3β inactivation and β-catenin stabilization.[18] The latency-associated nuclear antigen of Kaposi's sarcoma-associated herpesvirus binds to GSK3β and sequesters it in the nucleus, preventing β-catenin phosphorylation.[31] Previously, Shackelford *et al.*[32] reported that β-catenin was activated in type III EBV-infected B lymphocytes. They found that β-catenin is associated with deubiquitination of enzymes.[32] Another EBV encoding LMP2A also activates PI3K/AKT signaling, resulting in GSK3β inactivation and β-catenin stabilization in epithelial cells.[33] It is not clear at present which LMP (LMP1 or LMP2A) is more important in activation of β-catenin in B lymphocytes. The roles of LMP2A in the growth of EBV-immortalized B cells are currently being investigated in our laboratory.

In summary, the data presented here show that β-catenin is activated in EBV-immortalized B-cells. β-Catenin signaling had an important role in the growth of EBV-immortalized B-cells. LMP1 activated β-catenin through PI3K/AKT signaling, and LMP1 CTAR-1 domain was crucial for activation of this pathway (Fig. 4). Our results implicate LMP1 in the activation of the β-catenin signaling pathway and hence in the malignant growth of B lymphocytes following EBV infection.

Acknowledgments

We thank Dr B. Vogelstein for providing reporter plasmids pGL3-OT and pGL3-OF, Dr M. Rowe for providing LMP1 and LMP1 mutant plasmids, and Dr D. Alessi for the dominant-negative AKT. We also thank all members of our laboratories for the helpful comments and collaborations. This work was supported in part by grants-in-aid from the Ministry of Education, Culture, Sports, Science and Technology of Japan (No. 19591122); Takeda Science Foundation; and Japan Leukemia Research Fund; and a grant from the Princes Takamatsu Cancer Research Fund (No. 07-23905) and Kanehara Ichiro Memorial Foundation for Promotion of Medicine.

References

1 Rickinson AB, Kieff E. Epstein-Barr virus and its replication. *Fields Virology*, 4th edn. Philadelphia, PA: Lippincott Williams & Wilkins, 2006: 2655–700.
2 Kaye KM, Izumi KM, Kieff E. Epstein-Barr virus latent membrane protein 1 is essential for B-lymphocyte growth transformation. *Proc Natl Acad Sci USA* 1993; **90**: 9150–4.
3 Liebowitz D, Wang D, Kieff E. Orientation and patching of the latent infection membrane protein encoded by Epstein-Barr virus. *J Virol* 1986; **58**: 233–7.
4 Hammarskjold ML, Simurda MC. Epstein-Barr virus latent membrane protein transactivates the human immunodeficiency virus type 1 long terminal repeat through induction of NF-κB activity. *J Virol* 1992; **66**: 6496–501.
5 Paine E, Scheinman RI, Baldwin AS Jr, Raab-Traub N. Expression of LMP1 in epithelial cells leads to the activation of a select subset of NF-κB/Rel family proteins. *J Virol* 1995; **69**: 4572–6.
6 Izumi KM, Kieff ED. The Epstein-Barr virus oncogene product latent membrane protein 1 engages the tumor necrosis factor receptor-associated death domain protein to mediate B lymphocyte growth transformation and activate NF-κB. *Proc Natl Acad Sci USA* 1997; **94**: 12592–7.
7 Kieser A, Kilger E, Gires O, Ueffing M, Kolch W, Hammerschmidt W. Epstein-Barr virus latent membrane protein-1 triggers AP-1 activity via the c-Jun N-terminal kinase cascade. *EMBO J* 1997; **16**: 6478–85.
8 Eliopoulos AG, Blake SM, Floettmann JE, Rowe M, Young LS. Epstein-Barr virus-encoded latent membrane protein 1 activates the JNK pathway through its extreme C terminus via a mechanism involving TRADD and TRAF2. *J Virol* 1999; **73**: 1023–35.
9 Eliopoulos AG, Gallagher NJ, Blake SM, Dawson CW, Young LS. Activation of the p38 mitogen-activated protein kinase pathway by Epstein-Barr virus-encoded latent membrane protein 1 coregulates interleukin-6 and interleukin-8 production. *J Biol Chem* 1999; **274**: 16085–96.
10 Roberts ML, Cooper NR. Activation of a ras-MAPK-dependent pathway by Epstein-Barr virus latent membrane protein 1 is essential for cellular transformation. *Virology* 1998; **240**: 93–9.
11 Gires O, Kohlhuber F, Kilger E *et al.* Latent membrane protein 1 of Epstein-Barr virus interacts with JAK3 and activates STAT proteins. *EMBO J* 1999; **18**: 3064–73.
12 Luo J, Manning BD, Cantley LC. Targeting the PI3K-Akt pathway in human cancer: rationale and promise. *Cancer Cell* 2003; **4**: 257–62.
13 Dawson CW, Tramountanis G, Eliopoulos AG, Young LS. Epstein-Barr virus latent membrane protein 1 (LMP1) activates the phosphatidylinositol 3-kinase/Akt pathway to promote cell survival and induce actin filament remodeling. *J Biol Chem* 2003; **278**: 3694–704.
14 Mainou BA, Everly DN Jr, Raab-Traub N. Epstein-Barr virus latent membrane protein 1 CTAR1 mediates rodent and human fibroblast transformation through activation of PI3K. *Oncogene* 2005; **24**: 6917–24.
15 Polakis P. Wnt signaling and cancer. *Genes Dev* 2000; **14**: 1837–51.
16 Korinek V, Barker N, Morin PJ *et al.* Constitutive transcriptional activation by a β-catenin-Tcf complex in APC-/- colon carcinoma. *Science* 1997; **275**: 1784–7.
17 Morin PJ. β-catenin signaling and cancer. *Bioessays* 1999; **21**: 1021–30.
18 Tomita M, Kikuchi A, Akiyama T, Tanaka Y, Mori N. Human T-cell leukemia virus type 1 tax dysregulates β-catenin signaling. *J Virol* 2006; **80**: 10497–505.
19 Miller G, Lipman M. Comparison of the yield of infectious virus from clones of human and simian lymphoblastoid lines transformed by Epstein-Barr virus. *J Exp Med* 1973; **138**: 1398–412.
20 Tomita M, Choe J, Tsukazaki T, Mori N. The Kaposi's sarcoma-associated herpesvirus K-bZIP protein represses transforming growth factor β signaling through interaction with CREB-binding protein. *Oncogene* 2004; **23**: 8272–81.

21 Ishiyama M, Tominaga H, Shiga M, Sasamoto K, Ohkura Y, Ueno K. A combined assay of cell viability and in vitro cytotoxicity with a highly water-soluble tetrazolium salt, neutral red and crystal violet. *Biol Pharm Bull* 1996; **19**: 1518–20.
22 Kishida M, Hino S, Michiue T *et al.* Synergistic activation of the Wnt signaling pathway by Dvl and casein kinase Iε. *J Biol Chem* 2001; **276**: 33147–55.
23 Kishida S, Yamamoto H, Ikeda S *et al.* Axin, a negative regulator of the wnt signaling pathway, directly interacts with adenomatous polyposis coli and regulates the stabilization of β-catenin. *J Biol Chem* 1998; **273**: 10823–6.
24 Shih IMYuJ, He TC, Vogelstein B, Kinzler KW. The β-catenin binding domain of adenomatous polyposis coli is sufficient for tumor suppression. *Cancer Res* 2000; **60**: 1671–6.
25 Huen DS, Henderson SA, Croom-Carter D, Rowe M. The Epstein-Barr virus latent membrane protein-1 (LMP1) mediates activation of NF-κB and cell surface phenotype via two effector regions in its carboxy-terminal cytoplasmic domain. *Oncogene* 1995; **10**: 549–60.
26 Floettmann JE, Rowe M. Epstein-Barr virus latent membrane protein-1 (LMP1) C-terminus activation region 2 (CTAR2) maps to the far C-terminus and requires oligomerisation for NF-κB activation. *Oncogene* 1997; **15**: 1851–8.
27 Sharma M, Chuang WW, Sun Z. Phosphatidylinositol 3-kinase/Akt stimulates androgen pathway through GSK3β inhibition and nuclear β-catenin accumulation. *J Biol Chem* 2002; **277**: 30935–41.
28 Dawson CW, Laverick L, Morris MA, Tramoutanis G, Young LS. Epstein-Barr virus-encoded LMP1 regulates epithelial cell motility and invasion via the ERK-MAPK pathway. *J Virol* 2008; **82**: 3654–64.
29 Arron JR, Vologodskaia M, Wong BR *et al.* A positive regulatory role for Cbl family proteins in tumor necrosis factor-related activation-induced cytokine (trance) and CD40L-mediated Akt activation. *J Biol Chem* 2001; **276**: 30011–17.
30 Suzuki H, Terauchi Y, Fujiwara M *et al.* Xid-like immunodeficiency in mice with disruption of the p85α subunit of phosphoinositide 3-kinase. *Science* 1999; **283**: 390–2.
31 Fujimuro M, Wu FY, ApRhys C *et al.* A novel viral mechanism for dysregulation of β-catenin in Kaposi's sarcoma-associated herpesvirus latency. *Nat Med* 2003; **9**: 300–6.
32 Shackelford J, Maier C, Pagano JS. Epstein-Barr virus activates β-catenin in type III latently infected B lymphocyte lines: association with deubiquitinating enzymes. *Proc Natl Acad Sci USA* 2003; **100**: 15572–6.
33 Morrison JA, Klingelhutz AJ, Raab-Traub N. Epstein-Barr virus latent membrane protein 2A activates β-catenin signaling in epithelial cells. *J Virol* 2003; **77**: 12276–84.

doi: 10.1111/j.1349-7006.2009.01121.x

Available online at
ScienceDirect
www.sciencedirect.com

Elsevier Masson France
EM|consulte
www.em-consulte.com

BIOMEDICINE & PHARMACOTHERAPY

ELSEVIER MASSON

Biomedicine & Pharmacotherapy 63 (2009) 703–706

Point of View

Natural killer activity of peripheral-blood mononuclear cells in breast cancer patients

Md. Zahidunnabi Dewan [a,b,1,2], Masahiro Takada [c,1], Hiroshi Terunuma [d,e], Xuewen Deng [d], Sunjida Ahmed [a], Naoki Yamamoto [a,b], Masakazu Toi [c,*]

[a] *Department of Molecular Virology, Graduate School, Tokyo Medical and Dental University, 1-5-45 Yushima, Bunkyo-ku, Tokyo 113-8519, Japan*
[b] *AIDS Research Center, National Institute of Infectious Disease, 1-23-1 Toyama, Shinjuku-ku, Tokyo 162-8640, Japan*
[c] *Department of Breast Surgery, Graduate School of Medicine, Kyoto University, 54 Kawaracho, Shogoin, Sakyo-ku, Kyoto 606-8507, Japan*
[d] *Biotherapy Institute of Japan, 2-4-8 Edagawa, Koutou-ku, Tokyo 135-0051, Japan*
[e] *Tokyo Clinic Marunouchi Oazo mc, Shin-Marunouchi Center Building, 1-6-2 Marunouchi, Chiyoda-ku, Tokyo 100-0005, Japan*

Received 23 January 2009; accepted 11 February 2009
Available online 25 February 2009

Abstract

Natural killer (NK) activity of immune cells plays a central role in host defense against cancer and virus-infected cells. Natural cytotoxic activity of peripheral-blood mononuclear cells was assessed by a Calcein-AM release assay in 89 subjects. In the present study, we here demonstrated that NK activities of peripheral-blood mononuclear cells (PBMCs) from breast cancer patients were significantly lower as compared with that of healthy individuals. There were significant differences in the NK activities of PBMCs from HER2-negative breast cancer patients as compared with HER2-positive patients. Our results suggest that NK activity of PBMCs is lower in breast cancer indicating a role for immunological natural host defense mechanisms against cancer.

Keywords: NK activity; Breast cancer; NK cell; PBMCs

1. Introduction

Cancer metastasis is the result of several sequential steps and represents a highly organized, non-random and organ-selective process [1]. Immune cells and a wide number of molecules have been implicated to be responsible for the primary growth and metastatic property of cancer cells [2–5]. Breast cancer is characterized by a distinct pattern of metastasis involving regional lymph nodes, bone marrow, lung and liver.

Natural killer (NK) cells are large granular lymphocytes that mediate innate immunity against pathogens and tumors [6]. NK cells were originally discovered because of their ability to kill tumor and virally infected cells without exposure to the target cell antigens. One study showed that individuals with low natural cytotoxic activity of peripheral-blood lymphocytes are at a significantly higher risk of cancer, compared with those of median or high activity [7]. It has been reported that NK cells isolated from HIV-infected individuals are impaired in their ability to kill the virus-infected autologous cells [8–11]. NK cells are capable of mediating antibody-dependent cell cytotoxicity (ADCC) against antibody-coated targets via their expression of a low-affinity receptor for IgG (FcγRIII or CD16). The humanized version of the anti-HER2/neu mAb (Trastuzumab) exhibits improved binding affinity to the extracellular R domain of Her2/neu and mediates potent growth inhibitory activity against Her2/neu-overexpresssing cell lines and xenografts [12]. In murine models, experimental data have

* Corresponding author at: Department of Breast Surgery, Graduate School of Medicine, Kyoto University, 54 Kawaracho, Shogoin, Sakyo-ku, Kyoto 606-8507, Japan.
E-mail address: toi@kuhp.kyoto-u.ac.jp (M. Toi).
[1] M.Z. Dewan and M. Takada equally contribute to this report.
[2] Present address: Department of Pathology, New York University School of Medicine, 550 First Avenue, New York, NY 10016, USA.

0753-3322/$ - see front matter © 2009 Elsevier Masson SAS. All rights reserved.
doi:10.1016/j.biopha.2009.02.003